Azole Assisted C−H Bond Activation Promoted by an Osmium-Polyhydride: Discerning between N and NH

Beatriz Eguillor,[†] Miguel A. Esteruelas,*[,†] Israel Fernández,[‡] Mar Gómez-Gallego,[‡] Agustí Lledós,[§] Mamen Martín-Ortiz,[‡] Montserrat Oliván,[†] Enrique Oñate,[†] and Miguel A. Sierra*[,‡]

[†]Departamento de Química Inorgánica, Instituto de Síntesis Química y Catálisis Homogénea (ISQCH), Centro de Innovación en Química Avanzada (ORFEO-CINQA), Universidad de Zaragoza-CSIC, 50009 Zaragoza, Spain

[‡]Departamento de Química Orgánica, Facultad de Ciencias Químicas, Centro de Innovación en Química Avanzada (ORFEO-CINQA), Universidad Complutense, 28040 Madrid, Spain

[§]Departament de Química, Centro de Innovación en Química Avanzada (ORFEO-CINQA), Universitat Autònoma de Barcelona, 08193 Cerdanyola del Vallès, Spain

Ⓢ *Supporting Information*

ABSTRACT: The capacity of the hexahydride complex $OsH_6(P^iPr_3)_2$ (**1**) to discern between the nitrogen atom and the NH unit in the azole assisted aryl C−H bond activation has been investigated. Complex **1** reacts with 2-phenylimidazole to give $OsH_3\{\kappa^2\text{-}C,N\text{-}(C_6H_4\text{-imidazole})\}(P^iPr_3)_2$ (**2**), which has been characterized by X-ray diffraction analysis. The structure proves the higher affinity of the metal center for the N atom in the presence of the NH unit, which remains unchanged, and reveals that in the solid state the molecules of this complex form infinite chains by means of intermolecular asymmetric 3-center bifurcated dihydrogen bonds. In solution, ^{1}H-DOSY NMR experiments suggest that the association degree decreases as the temperature increases. The fused six-membered ring of benzimidazole weakens the NH bond, enhancing its reactivity. As a consequence, complex **1** cannot discern between the N atom and the NH unit of 2-phenylbenzimidazole. Thus, the treatment of **1** with this substrate leads to a mixture of $OsH_3\{\kappa^2\text{-}C,N\text{-}(C_6H_4\text{-benzimidazole})\}(P^iPr_3)_2$ (**3**) and the dinuclear species $(P^iPr_3)_2H_3Os(C_6H_4\text{-benzimidazolate})OsH(\eta^2\text{-}H_2)(P^iPr_3)_2$ (**4**). The latter is the result of a N-assisted *ortho*-C−H bond activation of the phenyl group promoted by 0.5 equiv of **1** and the N−H bond activation promoted by the remaining 0.5 equiv of hexahydride **1** along with the agostic coordination of the remaining *ortho*-C−H bond to the metal center of the unsaturated fragment $OsH(\eta^2\text{-}H_2)(P^iPr_3)_2$. The comparison of the redox properties of **3** and **4** suggests that the interaction between the metal centers in the dinuclear compound is negligible. The replacement of the NH group of the azoles by a sulfur atom does not modify the behavior of the substrates. Thus, the reactions of **1** with 2-phenylthiazole and 2-phenylbenzothiazole afford $OsH_3\{\kappa^2\text{-}C,N\text{-}(C_6H_4\text{-thiazole})\}(P^iPr_3)_2$ (**5**) and $OsH_3\{\kappa^2\text{-}C,N\text{-}(C_6H_4\text{-benzothiazole})\}(P^iPr_3)_2$ (**6**). In turn, complexes **2**, **3**, **5**, and **6** are phosphorescent.
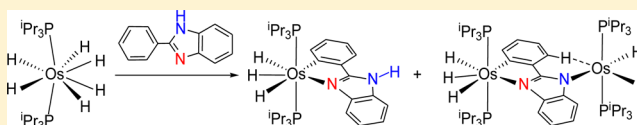
■ INTRODUCTION

The functionalization of a particular C−H bond requires its previous cleavage. Since the bond dissociation energies of the different C−H bonds are similar, it is hard to achieve a C−H bond cleavage in high conversion and high selectivity by thermal procedures. Transition-metals have the ability to enhance the reactivity of some parts of the organic molecules while inhibiting the reactions of others. Therefore, the use of transition-metal complexes is an excellent alternative to circumvent the selectivity problems encountered in C−H functionalization.[1]

The stability of metal complexes having two or more donor atoms in the same ligand is greater than when these atoms are placed on separated ligands. As a result, species having chelate rings are usually more stable than their nonchelated counterparts. Accordingly to this, among the different strategies available to stabilize particular transition-metal−carbon intermediates, the chelate-assistance strategy is considered to be one of the most efficient ways.[2] The assistance is performed by a coordination auxiliary (usually a coordinating heteroatom) present in an organic fragment, although the presence of different heteroatoms with similar affinity for a determined metal center necessarily provokes selectivity problems. In these cases, to know the coordination power of each heteroatom is essential to develop selective methods of C−H bond cleavage.

The hexahydride complex $OsH_6(P^iPr_3)_2$ is able to promote the cleavage of C−H bonds of a wide range of organic molecules.[3] The chelate-assistance strategy is crucial in these cases due to the high number of hydride ligands present in the hexahydride **1** that may favor the opposite process, namely the C−H bond formation. Among the coordination auxiliaries used, heterocyclic nitrogen atoms have been particularly helpful not only to perform the C−H bond activation of aromatic[4] and olefinic groups,[5] but also C(sp^3)-H bonds.[6]

In addition, this hexahydride complex activates N–H bonds of heterocycles such as 2,2′-biimidazole, pyrazole,[7] pyrrole[8] and pyrimidinic nucleobases,[9] being also the resulting nitrogen atom a good coordination auxiliary. The reaction conditions reported for the N–H activations are similar to those of C–H bond activations mediated by coordination with heterocyclic nitrogen atoms. In this regard, and in order to develop selective processes of C–H bond activation, we are interested in knowing the discrimination ability of the hexahydride complex OsH$_6$(P^{i}Pr$_3$)$_2$, between an aromatic nitrogen atom and the NH unit when are both placed in the same ring and the same C–H bond must be broken. With this aim, herein we have investigated the reactions of complex OsH$_6$(P^{i}Pr$_3$)$_2$ with 2-phenylimidazole and 2-phenylbenzimidazole. Furthermore, 2-phenylthiazole and 2-phenylbenzothiazole have been included in the study for comparative purposes, since the sulfur atom is isoelectronic with the NH unit (six-electrons), and it is a soft base showing affinity for soft metals such as osmium.[10]

Additionally, 1,3-azoles (imidazole, thiazole and their [benzo]derivatives) are relevant moieties in many luminescent organic compounds and their electronic properties have been exploited for a wide range of applications. Thus, imidazoles are structural motifs in metal–organic frameworks (MOFs)[11] or fluorescent dyes,[12] and thiazoles are found as part of π-functional and liquid-crystalline luminescent materials,[13] and their properties have been used by nature (bioluminescent insects)[14] and by man for the detection of specific types of biological processes by bioluminescence imaging.[15] The coordination ability of the azole nitrogen atom has resulted in their frequent incorporation as ligands in luminescent transition metal complexes, in particular of Ru(II),[16] Re(I)[17] or Ir(III),[18] in the construction of d^{10} mono- and polymetallic structures[19] and as sensors for anions or metal ions.[20] More recently, the role of benzimidazole as electron-transporting moiety has attracted the attention of researchers in the design of efficient host materials in phosphorescent organic light-emitting diodes.[21]

Considering these precedents, in this paper we show a study of the coordination auxiliary discrimination in the 1,3-azole assisted aromatic C–H bond activation promoted by the hexahydride complex OsH$_6$(P^{i}Pr$_3$)$_2$ and also explore the luminescent properties of the resulting Os(IV) complexes.[22]

■ RESULTS AND DISCUSSION

2-Phenylimidazole. Treatment of toluene solutions of the hexahydride complex OsH$_6$(P^{i}Pr$_3$)$_2$ (**1**) with 1.0 equiv of 2-phenylimidazole, under reflux, for 2.5 h leads to the trihydride derivative OsH$_3$\{κ^2-C,N-(C$_6$H$_4$-imidazole)\}(P^{i}Pr$_3$)$_2$ (**2**), as a result of the nitrogen assisted ortho-C–H activation of the phenyl group and the release of two hydrogen molecules (eq 1).
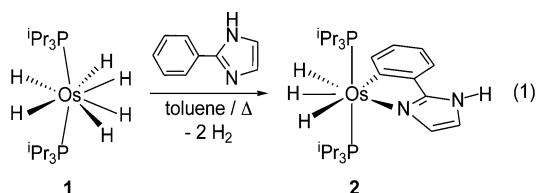
Complex **2** was isolated as a pale green solid in 67% yield and characterized by X-ray diffraction analysis. The structure (Figure 1) proves the higher affinity of the metal center for
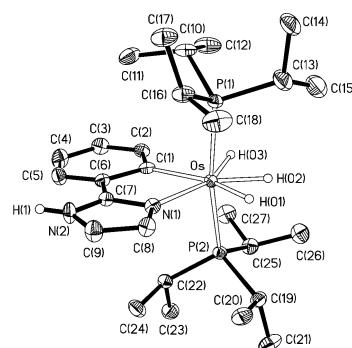
Figure 1. ORTEP diagram of complex **2** (50% probability ellipsoids). Hydrogen atoms (except hydrides and N–H) are omitted for clarity. Selected bond lengths (Å) and angles (deg): Os–N(1) = 2.157(2); Os–C(1) = 2.128(2); H(01)···H(02) = 1.56(4); H(02)···H(03) = 1.58(3); P(1)–Os–P(2) = 170.70(2); C(1)–Os–N(1) = 76.45(8).

the nitrogen atom in the presence of the NH unit, which remains unchanged. The geometry around the osmium atom can be rationalized as a distorted pentagonal bipyramid, with the phosphine ligands occupying axial positions (P(1)–Os–P(2) = 170.70(2)°). The metal coordination sphere is completed by the ortho-metalated ligand, which acts with a C(1)–Os–N(1) bite angle of 76.45(8)°, and the hydride ligands. H(01) and H(02) are separated by 1.56(4) (1.690 Å in the optimized structure), whereas H(02) and H(03) are separated by 1.58(3) (1.712 Å in the optimized structure). The Os–N(1) distance of 2.157(2) Å is similar to those found in lower π-electron osmacyclic nitrogen containing compounds,[23] whereas the Os–C(1) bond length of 2.128(2) Å compares well with the Os-aryl distances reported for other five-membered osmacycles resulting from orthometalation reactions.[24] In agreement with the presence of three inequivalent hydride ligands in the complex, the ^{1}H NMR spectrum (toluene-d_8, at 193 K) shows, in addition to the NH resonance at 8.55 ppm, three high field region signals at −6.86, −11.32, and −11.44 ppm, whereas the ^{31}P\{^{1}H\} NMR spectrum contains a singlet at 21.1 ppm, as expected for equivalent phosphines. The metalated aryl carbon atom gives rise to a triplet (J_{C-P} = 7.3 Hz) at 181.8 ppm in the ^{13}C\{^{1}H\} NMR spectrum.

An extended view of the structure (Figure 2) reveals that the molecules of the complex form infinite chains by means of intermolecular highly asymmetric 3-center bifurcated dihydrogen bonds,[25] involving the coordination of the imidazole NH-hydrogen of a molecule (H(1)), with two hydride ligands of the
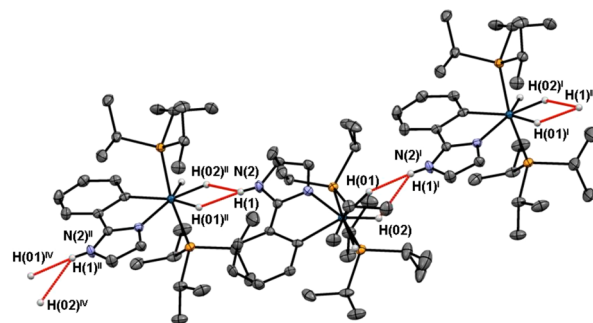
Figure 2. View of the interactions via hydrogen bonding in the structure of **2** [symmetry codes: (I) 1/2 − x, −1/2 + y, z; (II) 1/2 − x, 1/2 + y, z; (III) x, −1 + y, z; (IV) x, 1 + y, z.

neighbor: the central one (H(02)) and that disposed *transoid* to the metalated aryl carbon atom (H(01)). The N(2)−H(1) bond points toward the Os−H(01) bond, the angles Os−H(01)−H(1) and H(01)−H(1)−N(2) are 141(2)° and 174(2)°, respectively, whereas the angles Os−H(02)−H(1) and H(02)−H(1)−N(2) are 115(1)° and 137(2)°. Consistently, the H(1)−H(01) distance of 1.90(3) Å is significantly shorter than the H(1)−H(02) separation of 2.30(3) Å; the shorter being similar to the distances found in other N−H···H−M examples[26] while the longest is almost nonbonding.[27]

^{1}H NMR Diffusion-ordered spectroscopy ([1]H-DOSY) experiments were carried out in toluene-d_8,[28] between 296 and 203 K, in order to gain more insight into the association degree of the molecules in solution. Pulsed field gradient (PFG) NMR is a method for measuring diffusion rates, which provides information about the size of the molecules in solution.[29] Self-diffusion of a chemical species in a solvent depends on its molecular size and its hydrodynamic volume. According to this principle, molecular association can promote changes in self-diffusion coefficients, which can allow the detection of the presence of hydrogen-bonded species in solution.[30] Table 1 summarizes the obtained diffusion

Table 1. Diffusion Coefficient, Viscosity of Toluene, and Hydrodynamic Radius of 2 for Each Temperature

T (K)	D (10^{-10} m^2 s^{-1})^a	η of C$_7$H$_8$ (mPa)^b	R_H (Å)^c
298	8.71	0.517	4.84
283	5.83	0.641	5.54
273	5.08	0.765	5.14
263	4.37	0.798	5.52
253	2.90	1.067	5.98
243	2.68	1.084	6.11
233	1.54	1.280	8.64
223	0.92	1.510	11.8
213	0.66	1.810	13.0
203	0.42	2.181	16.2

^{a}Diffusion coefficient. ^{b}Viscosity of toluene from Santos et al. *J. Phys. Chem. Ref. Data.* **2006**, 35 (1), 1. ^{c}Hydrodynamic radius calculated using the Stokes−Einstein equation.

coefficient for each temperature along with the corresponding hydrodynamic radius, whereas Figure 3 shows the variation of the latter as a function of the temperature. The results reveal that the association degree decreases as the temperature increases. At 298 K, the obtained diffusion coefficient is 8.71 × 10^{-10} m^2·s^{-1}, which corresponds to a hydrodynamic radius of
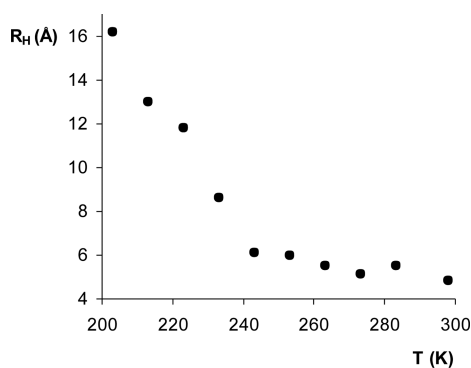

Figure 3. Hydrodynamic radius of **2** vs temperature.

4.84 Å. By means of the X-ray experiment, the calculated radius for **2** was 5.15 Å. Thus, the comparison of both values suggests that at this temperature the intermolecular H···H interaction is virtually broken. In addition, it should be mentioned that the formation and cleavage of the H···H interaction is very fast, since the hydride resonances are not affected by the hydrogen bond in the studied temperature range.

2-Phenylbenzimidazole. The N−H bond of benzimidazole is weakened respect to that of imidazole by the effect of the fused six-membered ring,[31] which enhances its reactivity. As a consequence, the hexahydride complex **1** cannot effectively discriminate between the nitrogen atom and the NH unit of 2-phenylbenzimidazole (Scheme 1). Thus, refluxing a toluene

Scheme 1
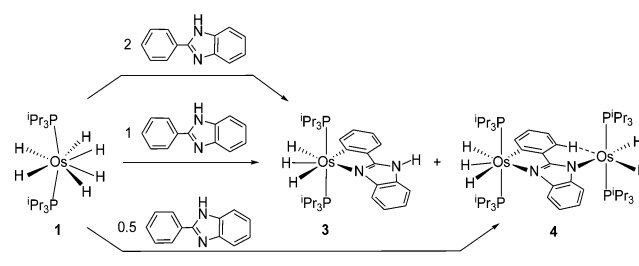
solution of **1** with 1.0 equiv of the substrate for 6 h leads to a mixture of the mononuclear derivative OsH$_3\{\kappa^2$-C,N-(C$_6$H$_4$-benzimidazole)}(P^{i}Pr$_3$)$_2$ (**3**) and a dinuclear species (P^{i}Pr$_3$)$_2$H$_3$Os(C$_6$H$_4$-benzimidazolate)OsH(η^2-H$_2$)(P^{i}Pr$_3$)$_2$ (**4**). Complex **3** is the benzimidazole counterpart of **2**, whereas the dinuclear species **4** is the result of two processes on the same substrate: a nitrogen assisted *ortho*-C−H bond activation of the phenyl group (as in **2** and **3**) promoted by 0.5 equiv of the starting compound and the N−H bond activation promoted by the remaining 0.5 equiv of hexahydride **1**. The two bond activations result in the release of two hydrogen molecules of each metal center. The removal of hydrogen from one of the Os-center generates a coordination vacancy that is saturated by agostic coordination of the remaining *ortho*-C−H bond of the phenyl substituent of the heterocycle. Furthermore, the Os-center involved in the agostic interaction undergoes a reduction process from trihydride to hydride−elongated dihydrogen (*vide infra*). Because the coordination of a C−H bond to an unsaturated metal fragment is the first step for its metal mediated cleavage,[32] the stabilization of the chelate N−CH agostic interaction can be viewed as a truncated activation event of the second *ortho*-C−H bond of the phenyl substituent.

Complex **3** is generated nearly quantitatively in the presence of 2 equiv of heterocycle (Scheme 1). Under these conditions it was isolated as a pale green solid in 53% yield. As in the case of complex **2**, at 193 K, the ^{1}H NMR spectrum of **3** in toluene-d_8 shows three hydride resonances at −7.07, −11.03, and −11.37 ppm, in addition to the NH signal at 8.33 ppm, whereas the ^{31}P{^{1}H} NMR spectrum contains a singlet at 21.2 ppm. In the ^{13}C{^{1}H} NMR spectrum, the resonance corresponding to the aryl metalated carbon atom appears at 184.6 ppm, as a triplet with a C−P coupling constant of 6.0 Hz.

The dinuclear complex **4** is the main reaction product when 0.5 equiv of 2-phenylbenzimidazole are used. It was isolated as a pure dark green solid in 60% yield and characterized by X-ray diffraction analysis. The structure (Figure 4) proves the dinuclear character of the compound, the nitrogen assisted *ortho*-C−H bond activation on a metal center (Os(1)) and the
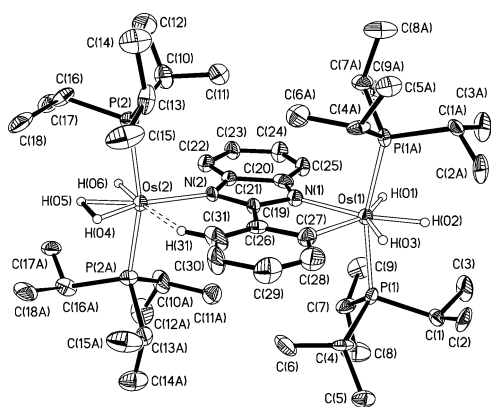
Figure 4. ORTEP diagram of complex **4** (50% probability ellipsoids). Hydrogen atoms (except hydrides and agostic C−H) are omitted for clarity. Selected bond lengths (Å) and angles (deg): Os(1)−N(1) = 2.189(7), Os(1)−C(27) = 2.223(11), Os(2)−N(2) = 2.098(7), Os(2)···H(31) = 2.16(7), Os(2)···C(31) = 3.06(1), C(31)−H(31) = 0.999(10), H(01)···H(02) = 1.99(1), H(02)···H(03) = 1.79(1), H(04)−H(05) = 1.29(1); P(1)−Os(1)−P(1A) = 163.04(17), N(1)−Os(1)−C(27) = 75.3(3), P(2)−Os(2)−P(2A) = 163.16(19).

N−H bond activation−agostic C−H coordination on the other one (Os(2)). The respective trihydride and hydride- elongated dihydrogen nature of the Os(1)H$_3$ and Os(2)H$_3$ units were confirmed by means of the Density Functional Theory (DFT) optimized structure at the M06/6-311G(d,p)&SDD(f) level (see Computational Details below). The coordination polyhedron around Os(1) can be described as a pentagonal bipyramid. The phosphine ligands occupy the axial positions (P(1)−Os(1)−P(1A) = 163.04(17)°) whereas the chelate unit (N(1)−Os(1)−C(27) = 75.3(3) °) and the hydride ligands, separated by 1.99(1) (1.707 Å in the optimized structure; H(01)−H(02)) and 1.79(1) (1.698 Å in the optimized structure; H(02)−H(03)) Å, lie in the equatorial plane. Although the Os(1)−N(1) and Os(1)−C(27) bond lengths of 2.189(7) and 2.223(11) Å, respectively, compare well with the corresponding ones in **2**, they are slightly longer. The geometry around Os(2) can be rationalized as a distorted octahedron, with *trans*-phosphines (P(2)−Os(2)−P(2A) = 163.16(19)°). The perpendicular plane is formed by the elongated dihydrogen (H(04)−H(05) = 1.29(1) Å; 1.323 Å in the optimized structure) *trans* disposed to the nitrogen atom N(2) and the hydride H(06) *trans* disposed to the C(31)−H(31) bond involved in the agostic interaction. The Os(2)−N(2) bond appears to be stronger than the Os(1)−N(1) one. Thus, the Os(2)−N(2) distance of 2.098(7) Å is about 0.09 Å shorter than the Os(1)−N(1) bond length. The Os(2)−C(31) and Os(2)−H(31) separations of 3.06(1) (3.055 Å in the optimized structure) and 2.16(7) Å (2.100 Å in the optimized structure), respectively, as well as the C(31)−H(31) distance of 0.999(10) Å (1.107 Å in the optimized structure) support the agostic interaction between the *ortho* C(31)−H(31) bond of the phenyl group and Os(2).[33] The r_{bd} value of 1.12 Å agrees well with those calculated for other δ agostic interactions.[34]

To gain more insight into the bonding situation of **4**, we also analyzed the C−H···Os agostic interaction with the help of the Atom in Molecules (AIM) and Natural Bond Orbital (NBO) methods. The laplacian distribution of **4** in the C−H···Os plane (Figure 5) clearly reveals the occurrence of a bond critical point between the transition metal and the hydrogen atom (pointed by two red arrows), which is associated with a bond path
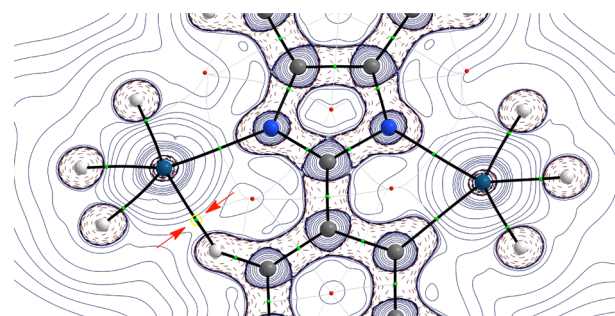

Figure 5. Contour line diagrams $\nabla^2\rho(r)$ for complex **4** in the Os−H−C plane. The solid lines connecting the atomic nuclei are the bond paths while the small green and red spheres indicate the corresponding bond critical points (BCP) and ring critical points (RCP), respectively. The BCP corresponding to the agostic interaction is indicated by two red arrows.

running between the corresponding two atoms. Moreover, the computed value of 0.032 e Å^{-3} for the electron density at the bond critical point is in the range reported for related CH agostic interactions.[35] This proves the existence of a direct interaction between both atoms and confirms the agostic nature of the bonding. In addition, further support to this finding is provided by the Second-Order Perturbation Theory (SOPT) of the NBO method, which locates a stabilizing electronic donation from the doubly occupied σ(C−H) molecular orbital to the vacant d atomic orbital of the osmium (associated second-order perturbation energy of −22.0 kcal·mol^{-1}).

The ^{1}H, ^{13}C{^{1}H} and ^{31}P{^{1}H} NMR spectra of **4** are consistent with the structure shown in Figure 4 and, in accordance with the r_{bd} value, confirm the strength of the agostic interaction that persists in toluene-d_8, at room temperature. In the ^{1}H NMR spectrum the most noticeable features are the hydride resonances and the signal corresponding to the hydrogen atom H(31) involved in the agostic interaction. At 203 K, the spectrum contains five resonances between −6 and −19 ppm (Figure 6). In agreement with **2** and
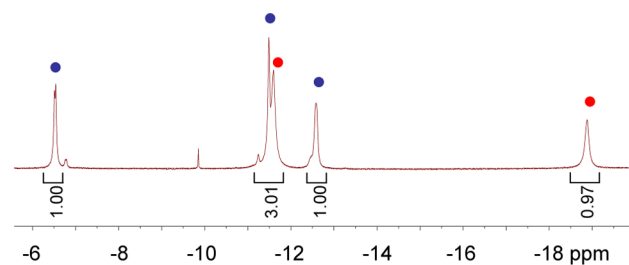

Figure 6. High field ^{1}H{^{31}P} NMR spectrum (400 MHz, C$_7$D$_8$, 203 K) of complex **4**. Blue dots: resonances assigned to the Os(1)H$_3$ unit. Red dots: resonances assigned to the Os(2)H$_3$ unit.

3, those corresponding to the trihydride Os(1)H$_3$ unit are observed at −6.54, - 11.49 and −12.60 ppm, whereas those due to the elongated dihydrogen−hydride Os(2)H$_3$ unit appear at −11.60 (H2) and −18.90 (H) ppm. At room temperature, the signal corresponding to H(31) is observed at 1.47 ppm, an unusually high field for an aryl resonance. The ^{1}H−^{1}H COSY NMR spectrum (Figure 7) shows the cross-peak of this signal with the aromatic signal at 6.88 ppm. In a consistent manner, the ^{13}C{^{1}H} NMR spectrum also shows the resonance due to C(31), involved in the agostic interaction, at unusually high field (108.6 ppm). Furthermore, the INEPT ^{13}C spectrum
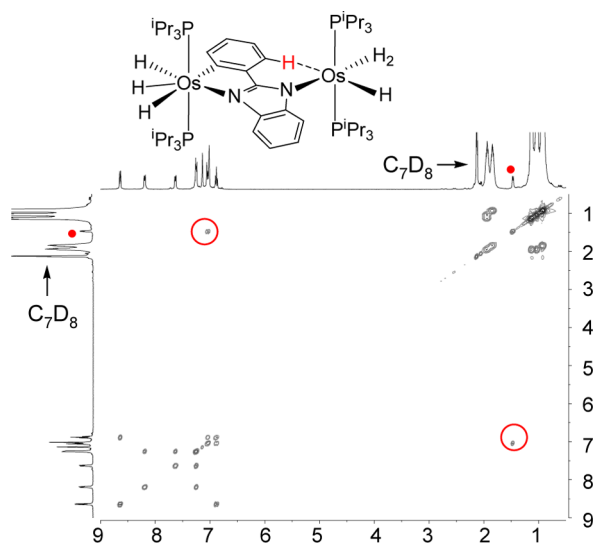
Figure 7. Partial view of the $^1H–^1H$ COSY NMR spectrum (400 MHz, C_7D_8, 298 K) of **4** showing the cross peaks between the resonance at 1.47 ppm (C–H agostic) and one of the protons of the metalated phenyl group.

Figure 8. (a) Cyclic voltammetries (CV) and (b) Osteryoung square-wave voltammetries (SW) for complexes **3** and **4** (10^{-3} M acetonitrile solutions, containing 0.1 M $[N(^nBu)_4]ClO_4$ as supporting electrolyte at 20 °C).

shows a C–H coupling constant of 121.3 Hz for that signal, which is about 40 Hz lower than the other phenyl $^1J_{C-H}$ coupling constants. The phenyl metalated C(27) resonance appears at 180.6 ppm, as a triplet with a C–P coupling constant of 7 Hz, in agreement with **2** and **3**. The $^{31}P\{^1H\}$ NMR spectrum contains two singlets at 35.7 and 21.6 ppm, corresponding to the Os(2)P_2 and Os(1)P_2 units, respectively.

The comparison of the spectroscopic data of **3** and **4** suggests that the influence between the metal centers in the dinuclear complex is very scarce, since the spectroscopic features of the moiety associated with Os(1) are almost identical to those of **3**. This assumption was confirmed by the study of the redox properties of both compounds. Cyclic voltammetries (CV) and Osteryoung square-wave voltammetry (SW) were conducted in acetonitrile utilizing concentrations 10^{-3} M of the test sample and 0.1 M of the supporting electrolyte $[N(^nBu)_4]ClO_4$. Results are summarized in Table 2, whereas CV's and SW's are shown in Figure 8.

Table 2. Cyclic Voltammetry Data of Complexes 3 and 4[a]

Compd	E_1	E_2[b] (ΔE)	E_3	E_4[b] (ΔE)	E_5
3	0.22	0.43 (90)	0.95	1.42 (100)	
4	0.20	0.44 (60)	0.97	1.42 (80)	1.75
2-phenyl benzimidazole	1.51				

[a]Data obtained from 10^{-3} M acetonitrile solutions, containing 0.1 M $[N(^nBu)_4]ClO_4$ as supporting electrolyte at 20 °C. Data are given in mV. Potentials are relative to Ag/AgCl. [b]$E_{1/2}$ values.

Data in Table 2 indicate that compounds **3** and **4** have almost identical electrochemical behavior, showing four main oxidation events at similar E_{pa} values. Taking into account that compound **4** has two metal centers in two different *formal* oxidation states [Os(1)(IV) and Os(2)(II)] these results deserve further comments. To gain more information about the process DFT calculations at M06/6-311G(d,p)&SDD(f) level were performed on both compounds. Figure 9 depicts the HOMO orbitals (closed shell species) and the spin densities
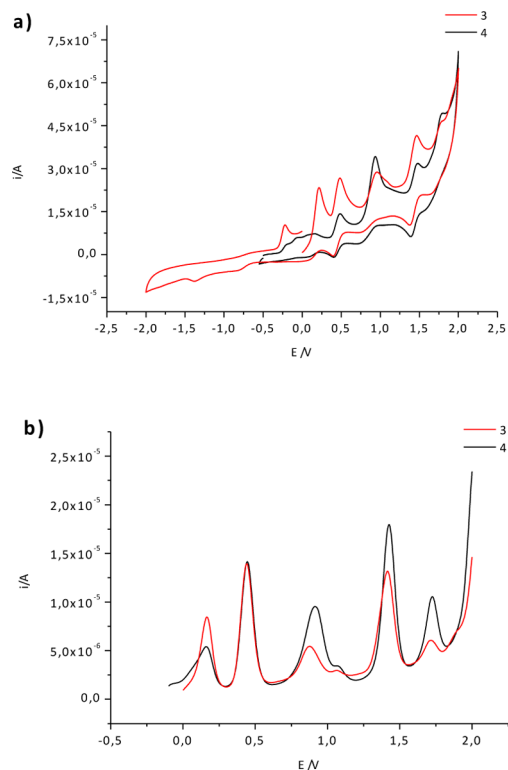
(open shell species) of the different compounds formed after the successive loss of electrons from mono- and dinuclear compounds **3** and **4**. In agreement with the CV results, the similarity between both complexes along the oxidation process is also apparent in the DFT calculations. Undoubtedly in dinuclear complex **4** the Os(1) unit plays the main role in the sequential loss of electrons and the presence of the additional metal fragment is only perceived after the formation of the trication $[4]^{3+}$, in which the spin density (0.71e) is mainly placed on the Os(2). The electrochemical behavior observed for mono- and dinuclear complexes **3** and **4** is fully consistent with the similitudes found in both, orbital distribution and energy, not just for the HOMO orbitals in Figure 9 (−4.80 eV for **3** and −4.98 eV for **4**) but also for the HOMO−1 and HOMO−2 orbitals (see Supporting Information). In fact, the OsH(η^2-H_2)(P^iPr_3)$_2$ moiety can be considered more a part of the benzimidazole ligand than an independent metal fragment.

The structural changes produced during the oxidation events give more details about the insights of the process (Figure 10). The optimized structures reveal how the successive oxidations cause the approaching of H(02) to H(03). In the case of the mononuclear complex **3**, the separation between the hydrides H(02) and H(03) changes from 1.75 Å in **3** to 1.52 Å in monocation $[3]^+$ and to 0.87 Å in the dication $[3]^{2+}$, that becomes a hydride-dihydrogen species. For the dinuclear compound, the H(02)–H(03) shortening goes from 1.70 Å in **4** to 0.85 Å in $[4]^{2+}$. By contrast, and in agreement with the spectator role of the fragment associated with Os(2), the hydride-elongated dihydrogen nature of the Os(2)H_3 unit is maintained with little changes during the successive oxidations, although finally the H(04)–H(05) bond length is reduced from
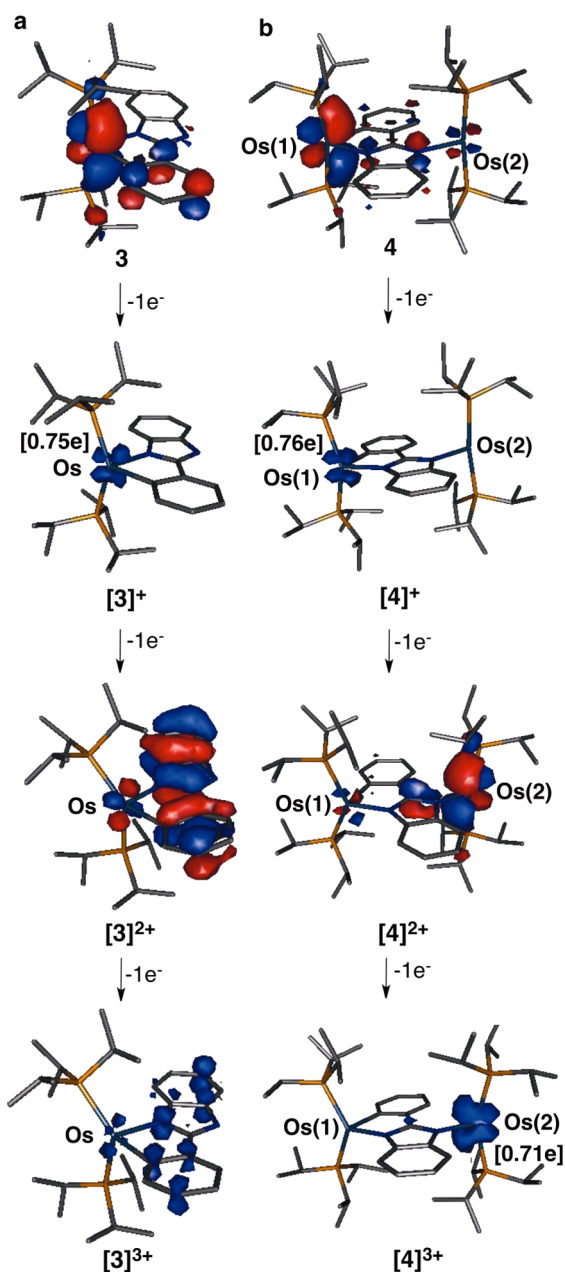
Figure 9. Sequential oxidation of mononuclear complex **3** (a) and dinuclear complex **4** (b). The figure shows the computed HOMO orbitals of complexes **3** and **4** and dications [**3**]$^{2+}$ and [**4**]$^{2+}$ (isosurface values 0.04) and the spin densities of monocations [**3**]$^+$ and [**4**]$^+$ and trications [**3**]$^{3+}$ and [**4**]$^{3+}$ (isosurface values 0.028) (in brackets computed Mulliken-spin densities). H atoms are omitted for clarity. All data have been computed at the M06/6-311G(d,p)&SDD(f) level.
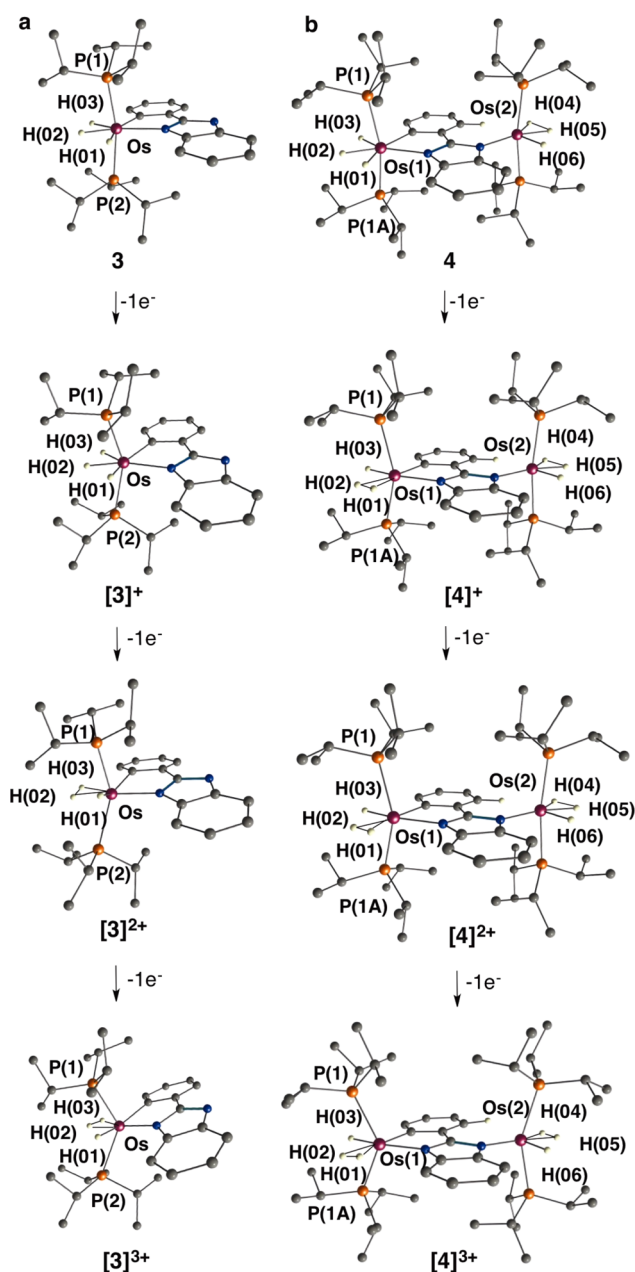

Figure 10. Optimized geometries (computed at the M06/6-311G(d,p) &SDD(f) level) for the species formed during the sequential oxidation of mononuclear complex **3** (a) and dinuclear complex **4** (b). H were omitted for clarity, with exception made of the hydride positions.

1.32 Å in **4** to 0.89 Å in the trication [**4**]$^{3+}$. Additionally, the successive oxidations are accompanied by a reduction of the P—Os—P angle, from 164.3° in **3** to 132.4° in [**3**]$^{2+}$ (P(1)—Os(1)—P(2) angle in Figure 10a) and from 165.7° in **4** to 134.6° in [**4**]$^{2+}$ (P(1)—Os(1)—P(1A) angle in Figure 10b).

In this context it should be noted that [**3**]$^{2+}$ is a six-coordinate unsaturated species of a d^4-ion and Os(1) and its associated ligands form in [**4**]$^{2+}$ a similar metal fragment. It is well-known that the octahedral geometry is not favored for a heavy d^4 ion, which prefers to be diamagnetic. Thus, these compounds undergo a distortion that destabilizes one orbital from the t_{2g} set and simultaneously stabilizes some occupied

orbitals.[36] In agreement with this, the coordination polyhedron around [**3**]$^{2+}$ and Os(1) in [**4**]$^{2+}$ strongly deviates from a octahedron while remembers that of the cation [OsH(κ-N,N-o-HNC$_6$H$_4$NH)(CH$_3$CN)(P^{i}Pr$_3$)$_2$]$^{+}$[37] and members of the OsH$_2$Cl$_2$(P^{i}Pr$_3$)$_2$ family.[38] The hydride-dihydrogen transformation is a tautomerization equilibrium, which is consistent with the reversibility of the second oxidation wave. In this context, it should be noted that tha oxidation from **3** to [**3**]$^{2+}$ and from **4** to [**4**]$^{2+}$ is in fact the oxidation of two hydrides to afford a hydrogen molecule, keeping the metal centers their initial oxidation states. The subsequent third and four oxidation processes must be ligand dependent, which could be related to the high electron donor character of the benzimidazole fragment. This point is supported by the different electro-

chemical behavior found in other structurally related mono- and trinuclear trihydride-osmium(IV) complexes derived from 2-phenylpyridine ligands, in which only two metal-centered monoelectronic oxidation events were observed.[4c]

2-Phenylthiazole and 2-Phenylbenzothiazole. In spite of the soft nature of the sulfur atom of these molecules and the late third row transition-metal, they react with the hexahydride complex in the same manner as 2-phenylimidazole. Thus, treatment of toluene solutions of the hexahydride complex **1** with 1.0 equiv of 2-phenylthiazole and 2-phenylbenzothiazole under reflux leads to OsH$_3$$\{\kappa^2$-$C,N$-$(C_6H_4$-thiazole)$\}$(P^{i}Pr$_3$)$_2$ (**5**) and OsH$_3$$\{\kappa^2$-$C,N$-$(C_6H_4$-benzothiazole)$\}$(P^{i}Pr$_3$)$_2$ (**6**), which were isolated as orange and red solids in 56% and 76% yields, respectively (Scheme 2). The *N*-coordination was

Scheme 2
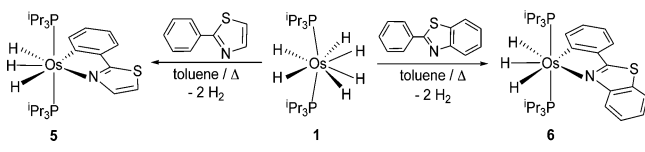
confirmed by means of the X-ray structures of both complexes (See Supporting Information). Although accurate structural parameters could not be obtained due to the disorder in the perpendicular plane to the P−Os−P direction, resulting from the packing of the molecules with the *ortho*-metalated ligand at 50% in its two possible orientations, the structures unambiguously demonstrate the nitrogen coordination and the pentagonal bipyramidal geometry around the osmium atom with *trans*-arrangement of the phosphines. DFT calculation for **5** show that the obtained isomer is 20.1 kcal·mol^{-1} more stable than that coordinated by the sulfur atom. The presence of three inequivalent hydride ligands in these compounds is strongly supported by their ^{1}H NMR spectra (toluene-d_8, 193 K), which show three hydride resonances (1:1:1 ratio) at −6.65, −11.35, and −11.45 for **5** and −6.32, −11.25, and −11.31 ppm for **6**. In agreement with the *trans*-disposition of the phosphine ligands, the ^{31}P$\{^1$H$\}$ NMR spectra contain a singlet at about 21 ppm. A triplet in the ^{13}C$\{^1$H$\}$ NMR spectra ($J_{C-P} \approx 6.5$ Hz) at about 187 ppm, corresponding to the aryl metalated carbon atom, is also a characteristic feature for these compounds.

The electrochemical behavior of 2-phenylbenzothiazole derivative **6** was similar to that of the parent compound **3**, showing four main oxidation events at E_{pa} values of 0.09, 0.43 ($E_{1/2}$), 0.41 and 1.44 V respectively (see Supporting Information).

Photophysical Properties. Absorption spectra of 1×10^{-5} M dichloromethane solutions of these compounds, at 298 K, show a similar profile (See Figure S5, Supporting Information). They exhibit two main absorption bands at the visible region: an intense absorption between 260 and 330 nm and a less intense band at lower energy (370−450 nm).

Time-dependent DFT calculations were performed in order to gain deeper insight into the electronic properties of the transitions involved in the absorption process in dichloro-methane. A very good agreement between the vertical excitation energies and the wavelengths of the absorption maxima in the experimental spectra was found, which allows the accurate assignment of the experimental observed bands (Table 3). Calculations indicate that the bands in the range 370−540 nm are the result of a combination of two one-

Table 3. UV/Vis Experimental Data (Recorded at Room Temperature in Dichloromethane with a Concentration 1 × 10^{-5} M) and Computed TD-B3LYP/6-311G(d,p) &SDD(f)//M06/6-311G(d,p)&SDD(f) Gas Phase Vertical Excitation Energies (the Value Corresponding to the Oscillator Strength, *f*, Is Given in Parentheses)

Complex	Obs λ [nm] (ε [×10^4 M^{-1} cm^{-1}])	Calc λ [nm]
2	265 (1.50), 374 (0.25)	259 (0.197), 357 (0.027), 383 (0.019)
3	300 (3.30), 420 (0.31)	293 (0.187), 404 (0.0287), 435 (0.034)
5	286 (1.64), 425 (0.41)	298 (0.154), 407 (0.04), 472 (0.018)
6	290 (1.70), 457 (0.45)	308 (0.155), 429 (0.041), 483 (0.030)

electron promotions from the HOMO−1 and HOMO to the LUMO. As depicted in Figure 11 for **5**, both HOMO−1 and
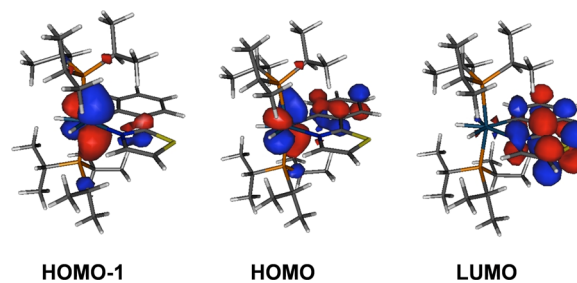

Figure 11. Computed HOMO−1, HOMO, and LUMO of complex **5** (isosurface value of 0.035 au).

HOMO should be viewed as d(π)-molecular orbitals which are mainly located at the metal whereas the LUMO is a π*-molecular orbital which is fully delocalized on the chelate ligand. So, the observed bands can be ascribed to metal-to-ligand charge transfer processes having a remarkable π−π* character.

The variations in the position of the MLCT band shown in Table 3 find their origin in the changes in the electronic nature of the chelate ligand attached to the osmium atom, which strongly affects the energy of the LUMO. Both the replacement of the NH group by a sulfur atom and the presence of a fused six-membered ring in the azole decrease the energy of the LUMO. In this context, it should be pointed out the good correlation between the position of the wavelength of the MLCT-absorption and the computed energy for the LUMO, which follows the sequence 374 nm (**2**; −0.77 eV) < 420 nm (**3**; −1.19 eV) < 425 nm (**5**; −1.79 eV) < 457 nm (**6**; −1.88 eV).

Complexes **2**, **3**, **5** and **6** are emissive upon photoexcitation, in the solid state and in toluene solution, at room temperature and at 77 K. Figure 12 depicts the emission spectra in the solid state (a) and in toluene (b) at room temperature. Lifetimes lie in the range 8−23 μs whereas the quantum yields are between 0.009 and 0.06 (Table 4).

In a consistent manner with the sequence of computed energy for the LUMO of the complexes, the energy of the emission decreases by replacement of the NH group by a sulfur atom and with the presence of a fused six-membered ring in the azole, i.e., in the sequence **2** > **3** > **5** > **6**. Thus, imidazole-derived complexes **2** and **3** are blue and green emissive,
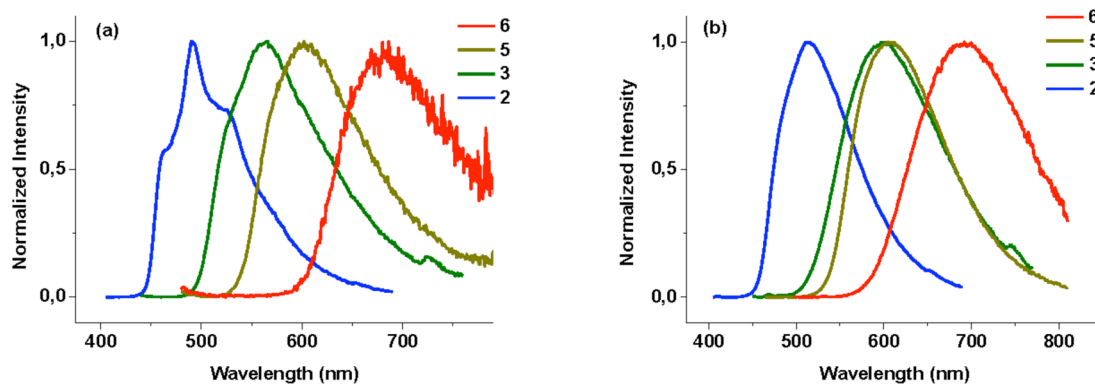
Figure 12. Emission for complexes **2**, **3**, **5** and **6** in solid state (a) and in toluene solutions (b) at room temperature.

Table 4. Photophysical Properties of Complexes 2, 3, 5, and 6 in the Solid State at 298 K and in Degassed Toluene at 298 and 77 K

Complex	media (T/K)	λ_{em} (nm)	τ (μs)	Φ^a
2	solid (298)	460, 490$_{max}$, 525 (λ_{exc} 365)	26.5	0.06
	C_7H_8 (298)	515 (λ_{exc} 365)	10.1	
	C_7H_8 (77)	470, 504$_{max}$, 543 (λ_{exc} 365)	22.8	
3	solid (298)	564 (λ_{exc} 400)	8.1	-^{c}
	C_7H_8 (298)	587 (λ_{exc} 410)	10.2	
	C_7H_8 (77)	581 (λ_{exc} 410)	17.5	
5	solid (298)	602 (λ_{exc} 440)	9.8	0.006
	C_7H_8 (298)	607 (λ_{exc} 425)	10.7	
	C_7H_8 (77)	588 (λ_{exc} 425)	15.5	
6	solid (298)	683 (λ_{exc} 440)	10.4	0.009
	C_7H_8 (298)	693 (λ_{exc} 457)	10.7	
	C_7H_8 (77)	654 (λ_{exc} 480)	-^{b}	

^{a}Measurements in solid state by doping 5% sample in PMMA film. ^{b}Too weak to be measured. ^{c}Decomposes.

respectively. For **2**, the spectrum in the solid state contains an intense band at 490 nm, and two shoulders at 460 and 525 nm, whereas in toluene at room temperature an intense band is observed at 515 nm. Because the intermolecular NH···hydride interactions discussed above (Figures 2 and 3) increase as the temperature decreases, the measured spectrum in toluene at 77 K is similar to that of the solid state (See Figures S7 and S6 of the Supporting Information), thus, it shows an intense band at 504 nm and two shoulders at 470 and 543 nm. The benzimidazole complex **3** shows an emission centered at 564 nm in the solid state and at 587 nm in toluene at room temperature. Although the NMR data and the redox properties of **3** and **4** are almost identical, suggesting that the influence between the metal centers in **4** is negligible, it should be mentioned that the replacement of the NH-hydrogen atom by the OsH(η^2-H$_2$)(P^{i}Pr$_3$)$_2$ metal fragment produces the quenching of the emissive properties. Taking into account the electrochemical properties of both compounds (see above), an intramolecular energy transfer mechanism rather than an electron transfer process could account for this observation.[39] The replacement of the NH of **2** and **3** by a sulfur atom produces new color shifts. The thiazol complex **5** is yellow emissive at about 600 nm, in both the solid state and in toluene, at room temperature and 77 K. Complex **6**, containing a benzothiazole assistant, is red emissive at about 680 nm, in the solid state. In toluene the bands are centered at 693 and 654 nm, at room temperature and 77 K, respectively.

Time-dependent DFT calculations on complex **2** indicate that the most stable excited state is a triplet (T$_1$), with a vertical excitation energy of 2.87 eV, the first singlet (S$_1$) resting 0.37 eV above T$_1$. These data are in agreement with an efficient S$_1$-T$_1$ intersystem crossing (ISC).[40] The computed spin densities on the optimized structure of this triplet state indicate that the unpaired electrons are located on the osmium atom (0.38 e) and on the chelate ligand (see Figure 13). Therefore, the
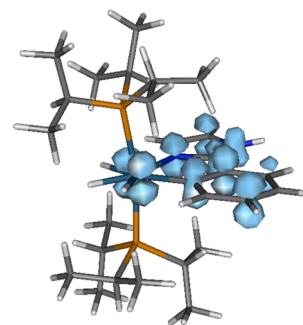

Figure 13. Computed spin density in the triplet state of **2**.

LUMO is populated in the most stable triplet state and, as a consequence, the trend observed in the wavelengths of the emission maxima is similar to that found in the UV/vis absorptions.

The emission wavelength can be roughly estimated through the difference in energy between the optimized triplet excited state and the singlet ground state with the same geometry as the optimized triplet excited state.[41] Thus, we have computed the emission wavelength in the gas-phase for complex **2**. The obtained value is in good agreement with the experimental data: 572 nm (computed) versus 525 nm (experimental, see Table 4). The comparison strongly supports that the observed luminescence is the result of the emission from the most stable triplet excited state.

■ CONCLUDING REMARKS

This study shows the capacity of the hexahydride complex OsH$_6$(P^{i}Pr$_3$)$_2$ to discern between the nitrogen atom and the NH unit in the azole assisted C−H bond activation. This complex selectively promotes the nitrogen assisted *ortho*-C−H bond activation of the phenyl group of 2-phenylimidazole to afford an OsH$_3$\{κ^2-*C*,*N*-(C$_6$H$_4$)-azole\}(P^{i}Pr$_3$)$_2$ derivative. The presence of a fused six-membered ring in the azole weakens the N−H bond. As a consequence, the hexahydride complex

cannot discern completely between the nitrogen atom and the NH unit. Thus, in contrast to 2-phenylimidazole, 2-phenyl-benzimidazole reacts with the hexahydride to give a mixture of two compounds: the corresponding $OsH_3\{\kappa^2\text{-}C,N\text{-}(C_6H_4)\text{-}azole\}(P^iPr_3)_2$ derivative and a dinuclear species. The latter is the result of two processes on the same substrate: a nitrogen assisted *ortho*-C−H bond activation of the phenyl group promoted by 0.5 equiv of the starting compound and the N−H bond activation promoted by the remaining 0.5 equiv of hexahydride joined with the agostic coordination of the remaining phenyl *ortho*-C−H bond. The spectroscopic data and electrochemical behavior of this compound indicate that the mutual influence between the metal centers is negligible. The replacement of the NH group of the azole by a sulfur atom does not modify the behavior of the substrates, in spite of the soft character of the sulfur atom and the late third row transition metal. Thus, 2-phenylthiazole and 2-phenylbenothia-zole react as 2-phenylimidazole, affording also the selective nitrogen assisted C−H bond activation of the phenyl group.

Complexes $OsH_3\{\kappa^2\text{-}C,N\text{-}(C_6H_4)\text{-}azole\}(P^iPr_3)_2$ show phosphorescence upon photoexcitation. The emission energy decreases as a consequence of the replacement of the NH unit by a sulfur atom and the presence of a fused six-membered ring in the azole. This is related to the decrease of the energy of the LUMO of the resulting compounds, which is mainly centered on the chelate ligand.

In conclusion, although the capacity to discern depends upon the strength of the N−H bond, in general, the hexahydride complex $OsH_6(P^iPr_3)_2$ shows preference by the nitrogen assisted C−H bond activation. The resulting $OsH_3\{\kappa^2\text{-}C,N\text{-}(C_6H_4)\text{-}azole\}(P^iPr_3)_2$ derivatives are novel examples of phosphorescent d^4-osmium emitters upon photoexcitation.

■ EXPERIMENTAL SECTION

General Information. All reactions were carried out with rigorous exclusion of air using Schlenk-tube techniques. Toluene was obtained oxygen- and water-free from an MBraun solvent purification apparatus. Methanol was dried and distilled under argon. ^1H, $^{31}P\{^1H\}$ and $^{13}C\{^1H\}$ NMR spectra were recorded on Bruker 300 ARX, Bruker Avance 300 MHz, and Bruker Avance 400 MHz instruments. Chemical shifts (expressed in parts per million) are referenced to residual solvent peaks (^1H, $^{13}C\{^1H\}$) or external 85% H_3PO_4 ($^{31}P\{^1H\}$). Coupling constants J and N are given in hertz. Attenuated total reflection infrared spectra (ATR-IR) of solid samples were run on a PerkinElmer Spectrum 100 FT-IR spectrometer. C, H, and N analyses were carried out in a PerkinElmer 2400 CHNS/O analyzer. High-resolution electrospray mass spectra were acquired using a MicroTOF-Q hybrid quadrupole time-of-flight spectrometer (Bruker Daltonics, Bremen, Germany). $OsH_6(P^iPr_3)_2$[38a] and 2-phenylthiazole[42] were prepared by published methods.

Photophysical Studies. All the manipulations of the organo-metallic compounds were carried out in strict absence of oxygen and water. UV−vis spectra were recorded on an Evolution 600 spectrophotometer. Steady-state photoluminescence spectra were recorded in a Jobin-Yvon Horiba Fluorolog FL-3-11 spectrofluor-ometer. An IBH 5000F coaxial nanosecond flash lamp was used to measure the lifetimes.

Reaction of $OsH_6(P^iPr_3)_2$ (1) with 2-Phenylimidazole: Preparation of $OsH_3\{\kappa^2\text{-}C,N\text{-}(C_6H_4)\text{-}imidazole\}(P^iPr_3)_2$ (2). A solution of **1** (150 mg, 0.290 mmol) in toluene (10 mL) was treated with 1.0 eq of 2-phenylimidazole (41.8 mg, 0.290 mmol). The resulting solution was heated at 120 °C for 2.5 h. During this time the color of the solution changed from colorless to greenish. The solution was filtered through Celite and was taken to dryness. The addition of methanol caused the precipitation of a pale green solid, which was washed with methanol and dried in vacuo. Yield: 128 mg (67%). Anal.

Calcd for $C_{27}H_{52}N_2OsP_2$: C, 49.37; H, 7.98; N, 4.27. Found: C, 48.97; H, 7.52; N, 4.38. HRMS (electrospray, *m/z*): calcd for $C_{27}H_{51}N_2OsP_2$ $[M − H]^+$ 657.3138, found 657.3132. IR (Nujol, cm^{-1}): ν(Os−H) 2167 (w). ^1H NMR (400 MHz, C_7D_8, 298 K): δ 8.68 (d, J_{H-H} = 7.3, 1H, Ph), 8.55 (br s, 1H, N−H), 7.72 (dd, J_{H-H} = 7.3, J_{H-H} = 1.3, 1H, Ph), 7.32 (d, J_{H-H} = 1.3, 1H, im), 7.11 (m, 1H, Ph), 6.97 (m, 1H, Ph), 6.19 (d, J_{H-H} = 1.3, 1H, im), 1.86 (m, 6H, PCH(CH$_3$)$_2$), 1.07 (dvt, J_{H-H} = 6.9, N = 12.3, 18H, PCH(CH_3)$_2$), 1.03 (dvt, J_{H-H} = 6.9, N = 12.3, 18H, PCH(CH_3)$_2$), −9.50 (br, 2H, OsH), −11.17 (br, 1H, OsH). $^1H\{^{31}P\}$ NMR (400 MHz, C_7D_8, 193 K, hydride region): δ −6.86 (br, 1H, OsH), −11.32 (br, 1H, OsH), −11.44 (br, 1H, OsH). $^1H\{^{31}P\}$ NMR (400 MHz, C_7D_8, 363 K): δ −10.14 (br, 3H, OsH). $^{31}P\{^1H\}$ NMR (161.90 MHz, C_7D_8, 298 K): δ 21.1.(s). $^{13}C\{^1H\}$ NMR (100.56 MHz, C_7D_8, 298 K, plus apt): δ 181.8 (t, J_{C-P} = 7.3, Os−C), 158.2 (s, NCN), 147.0 (s, CH Ph), 134.3 (s, C$_q$ Ph), 133.7 (s, CH im), 125.3, 121.1, 117.9 (all s, CH Ph), 114.4 (s, CH im), 27.3 (vt, N = 23.4, PCH(CH$_3$)$_2$), 19.8, 19.6 (both s, PCH(CH$_3$)$_2$). $T_{1(min)}$ (ms, OsH, 300 MHz, C_7D_8, 248 K): 90 (−9.34 ppm), 114 (−11.57 ppm).

Reaction of $OsH_6(P^iPr_3)_2$ (1) with 1 equiv of 2-Phenyl-benzimidazole. A solution of **1** (150 mg, 0.290 mmol) in toluene (10 mL) was treated with the 1.0 eq of 2-phenylbenzimidazole (56.3 mg, 0.29 mmol). The resulting solution was heated at 120 °C for 2 h. After this time a $^{31}P\{^1H\}$ NMR spectrum was recorded, showing that the solution contains a mixture of complexes **3** and **4** in a ratio 5 to 1.

Reaction of $OsH_6(P^iPr_3)_2$ (1) with 2.0 equiv of 2-Phenyl-benzimidazole: Preparation of $OsH_3\{\kappa^2\text{-}C,N\text{-}(C_6H_4)\text{-}benzimidazole\}(P^iPr_3)_2$ (3). A solution of **1** (150 mg, 0.290 mmol) in toluene (10 mL) was treated with 2.0 eq of 2-phenylbenzimidazole (112.7 mg, 0.58 mmol). The resulting solution was heated at 120 °C for 6 h. During this time the color of the solution changed from colorless to dark green. After cooling at room temperature, the solution was filtered through Celite and was taken to dryness. The addition of methanol caused the precipitation of a green solid, which was washed with methanol and dried in vacuo. Yield: 110 mg (53%). Anal. Calcd for $C_{31}H_{54}N_2OsP_2$: C, 52.67; H, 7.70; N, 3.96. Found: C, 52.34; H, 7.87; N, 4.08. HRMS (electrospray, *m/z*): calcd for $C_{31}H_{53}N_2OsP_2$ $[M − H]^+$ 707.3295, found 707.3277. IR (cm^{-1}): ν(OsH) 2072 (w). ^1H NMR (300 MHz, C_6D_6, 298 K): δ 8.82 (d, J_{H-H} = 7.4, 1H, Ph), 8.38 (d, J_{H-H} = 8.0, 1H, Ph), 8.33 (br, 1H, N−H), 7.34 (d, J_{H-H} = 7.0, 1H, Ph), 7.25 (t, J_{H-H} = 7.4, 1H, Ph), 7.09 (m, 3H, Ph), 6.98 (d, J_{H-H} = 8.0, 1H, Ph), 1.81 (m, 6H, PCH(CH$_3$)$_2$), 0.94 (m, 36H, PCH(CH_3)$_2$), −9.28 (br, 2H, OsH), −11.33 (br, 1H, OsH). $^1H\{^{31}P\}$ NMR (300 MHz, C_7D_8 193 K, hydride region): δ −7.07 (d, J_{H-H} = 23.6, 1H, OsH), −11.03 (br, 1H, OsH), −11.37 (d, J_{H-H} = 23.6, 1H, OsH). $^1H\{^{31}P\}$ NMR (300 MHz, C_7D_8, 353 K, hydride region): δ −10.11 (br, 3H, OsH). $^{31}P\{^1H\}$ NMR (121.42 MHz, C_6D_6, 298 K): δ 21.2 (s). $^{13}C\{^1H\}$ NMR (75.41 MHz, C_6D_6, 298 K, plus apt): δ 186.4 (t, J_{C-P} = 6.0, Os−C), 162.7 (s, NCN), 147.2 (s, CH Ph), 143.6, 133.4, 133.3 (all s, C$_q$), 126.8, 126.8, 123.4, 122.7, 121.7, 120.2, 118.2, 110.6 (all s, CH Ph and bzim), 27.2 (vt, N = 23.2, PCH(CH$_3$)$_2$), 20.0, 19.8 (both s, PCH(CH$_3$)$_2$). $T_{1(min)}$ (ms, OsH, 300 MHz, C_7D_8, 228 K): 109 (−11.20 ppm).

Reaction of $OsH_6(P^iPr_3)_2$ (1) with 0.5 equiv of 2-Phenyl-benzimidazole: Preparation of $(P^iPr_3)_2H_3Os(C_6H_4\text{-}benzimidazolate)OsH(\eta^2\text{-}H_2)(P^iPr_3)_2$ (4). A solution of **1** (162 mg, 0.310 mmol) in toluene (10 mL) was treated with the 0.5 eq of 2-phenylbenzimidazole (30.4 mg, 0.156 mmol). The resulting solution was heated at 120 °C for 6 h. During this time the color changed from colorless to dark green/brownish. After cooling at room temperature, the solution was filtered through Celite and was taken to dryness. The addition of methanol caused the precipitation of a dark green solid which was washed with methanol and dried in vacuo. Yield: 113 mg (60%). Anal. Calcd for $C_{49}H_{98}N_2Os_2P_4$: C, 48.25; H, 8.10; N, 2.30. Found: C, 48.65; H, 7.60; N, 1.96. IR (cm^{-1}): ν(OsH) 1953 (w), 2107 (w). ^1H NMR (400 MHz, C_7D_8, 298 K): δ 8.64 (d, J_{H-H} = 7.2, 1H, Ph), 8.19 (m, 1H, Ph), 7.63 (m, 1H, Ph), 7.24 (m, 2H, Ph), 7.04 (m, 1H, Ph), 6.88 (t, J_{H-H} = 7.2, 1H, Ph), 1.84 (m, 6H, PCH(CH$_3$)$_2$), 1.47 (d, J_{H-H} = 6, 1H, C$H_{agostic}$ Ph), 1.13 (dvt, J_{H-H} = 6.4, N = 12.1, 18H, PCH(CH_3)$_2$), 1.03 (dvt, J_{H-H} = 6.4, N = 12.1 18H, PCH(CH_3)$_2$), 0.92 (m, 36H, PCH(CH_3)$_2$), −9.50 (br, 2H, OsH), −11.68 (br, 1H, OsH),

−14.42 (br, 3H, OsH). $^1H\{^{31}P\}$ NMR (400 MHz, C_7D_8 203 K, hydride region): δ −6.54 (br d, J_{H-H} = 13, 1H, OsH), −11.49 (br, 1H, OsH), −11.60 (br, 2H, OsH), −12.60 (br, 1H, OsH), −18.90 (br s, 1H, OsH). $^{31}P\{^1H\}$ NMR (121.42 MHz, C_7D_8, 298 K): δ 35.7 and 21.6 (both s). $^{13}C\{^1H\}$ NMR (100.56 MHz, C_7D_8, 298 K, plus apt): δ 180.6 (t, J_{P-C} = 7.0, Os−C), 172.6 (s, NCN), 148.5 (s, CH Ph), 146.8, 144.5, 140.4 (all s, C_q), 127.2, 122.6, 119.5, 118.8, 118.7, 117.1 (all s, CH Ph and bzim), 108.6 (s, $CH_{agostic}$ Ph), 27.5 (vt, N = 26.0, $PCH(CH_3)_2$), 27.4 (vt, N = 22.8, $PCH(CH_3)_2$), 20.4, 20.0, 19.8 (all s, $PCH(CH_3)_2$).

Reaction of $OsH_6(P^iPr_3)_2$ (1) with 2-Phenylthiazole: Preparation of $OsH_3\{\kappa^2\text{-}C,N\text{-}(C_6H_4)\text{-thiazole}\}(P^iPr_3)_2$ (5). A solution of **1** (150 mg, 0.290 mmol) in toluene (10 mL) was treated with 1.0 eq of 2-phenylthiazole (46.8 mg, 0.290 mmol). The resulting solution was heated at 120 °C for 2.5 h. During this time the color of the solution changed from colorless to red. After cooling at room temperature, the solution was filtered through Celite and was taken to dryness. The addition of methanol caused the precipitation of an orange solid, which was washed with methanol and dried in vacuo. Yield: 110 mg (56%). Anal. Calcd for $C_{27}H_{51}NOsP_2S$: C, 48.12; H, 7.63; N, 2.08, S, 4.76. Found: C, 48.30; H, 7.57; N, 2.02; S, 5.02. HRMS (electrospray, m/z): calcd for $C_{27}H_{50}NOsP_2S$: $[M − H]^+$ 674.2747, found 674.2765. IR (Nujol, $cm^{−1}$): ν(OsH) 2153 (w). ^1H NMR (400 MHz, C_6D_6, 298 K): δ 8.85 (d, J_{H-H} = 7.4, 1H, Ph), 8.06 (d, J_{H-H} = 3.4, 1H, thiazole), 7.76 (dd, J_{H-H} = 7.4, J_{H-H} = 1.0, 1H, Ph), 7.14 (td, J_{H-H} = 7.4, J_{H-H} = 1.0, 1H, Ph), 7.08 (td, J_{H-H} = 7.4, J_{H-H} = 1.0, 1H, Ph), 6.33 (d, J_{H-H} = 3.4, 1H, thiazole), 1.89 (m, 6H, $PCH(CH_3)_2$), 1.10, (dvt, J_{H-H} = 6.8, N = 12.6, 18H, $PCH(CH_3)_2$), 1.05 (dvt, J_{H-H} = 6.8, N = 12.3, 18H, $PCH(CH_3)_2$), −9.08 (br, 2H, OsH), −11.60 (br, 1H, OsH). $^1H\{^{31}P\}$ NMR (400 MHz, C_7D_8, 183 K, hydride region): δ −6.65 (d, J_{H-H} = 30.5, 1H, OsH), −11.35 (d, J_{H-H} = 30.5, 1H, OsH), −11.45 (br, 1H, OsH). $^1H\{^{31}P\}$ NMR (400 MHz, C_7D_8, 353 K, hydride region): δ −9.95 (br, 3H, OsH). $^{31}P\{^1H\}$ NMR (161.90 MHz, C_6D_6, 298 K): δ 21.5 (s). $^{13}C\{^1H\}$ NMR (100.56 MHz, C_6D_6, 298 K, plus apt): δ 186.1 (t, J_{C-P} = 6.7, Os−C), 173.7 (s, NCN), 148.0, 145.6 (both s, CH Ph), 139.0 (s, C_q), 125.3, 127.7, 124.6, 113.7 (all s, CH Ph and thiazole), 26.2 (vt, N = 23.8, $PCH(CH_3)_2$), 18.7, 18.5 (both s, $PCH(CH_3)_2$). $T_{1(min)}$ (ms, OsH, 300 MHz, C_7D_8, 228 K): 54 (−6.71 ppm), 93 (−11.51 ppm).

Reaction of $OsH_6(P^iPr_3)_2$ (1) with 2-Phenylbenzothiazole: Preparation of $OsH_3\{\kappa^2\text{-}C,N\text{-}(C_6H_4)\text{-benzothiazole}\}(P^iPr_3)_2$ (6). A solution of **1** (150 mg, 0.290 mmol) in toluene (10 mL) was treated with 1.0 eq of 2-phenylbenzothiazole (61.3 mg, 0.290 mmol). The resulting solution was heated at 120 °C for 6 h. During this time the color of the solution changed from colorless to deep red. After cooling at room temperature, the solution was filtered through Celite and was taken to dryness. The addition of methanol caused the precipitation of a deep red solid, which was washed with methanol and dried in vacuo. Yield: 160 mg (76%). Anal. Calcd for $C_{31}H_{53}NOsP_2S$: C, 51.43; H, 7.38; N, 1.94; S, 4.43. Found: C, 51.05; H, 7.21; N, 1.80; S, 4.42. MS (MALDI+, m/z): $[M − 3H]^+$ 720.9. IR ($cm^{−1}$): ν(OsH) 2152 (w). ^1H NMR (400 MHz, C_6D_6, 298 K): δ 9.13 (d, J_{H-H} = 8.0, 1H, Ph), 8.80 (d, J_{H-H} = 7.3, 1H, Ph), 7.98 (d, J_{H-H} = 7.3, 1H, Ph), 7.35 (d, J_{H-H} = 8.0, 1H, Ph), 7.31 (t, J_{H-H} = 8.0, 1H, Ph), 7.06 (t, J_{H-H} = 7.3, 1H, Ph), 7.10 (t, J_{H-H} = 7.3, 1H, Ph), 6.99 (t, J_{H-H} = 8.0, 1H, Ph), 1.90 (m, 6H, $PCH(CH_3)_2$), 1.04 (dvt, J_{H-H} = 6.8, N = 12.7, 18H, $PCH(CH_3)_2$), 0.99 (dvt, J_{H-H} = 6.9, N = 12.4, 18H, $PCH(CH_3)_2$), −8.71 (br, 2H, OsH), −11.48 (br, 1H, OsH). $^1H\{^{31}P\}$ NMR (400 MHz, C_7D_8, 193 K, hydride region): δ −6.32 (br, 1H, OsH), −11.25 (br, 1H, OsH), −11.31 (br, 1H, OsH). $^1H\{^{31}P\}$ NMR (400 MHz, C_7D_8, 363 K, hydride region): δ −9.72 (br, 3H, OsH). $^{31}P\{^1H\}$ NMR (161.90 MHz, C_7D_8, 298 K): δ 21.4 (s). $^{13}C\{^1H\}$ NMR (100.56 MHz, C_6D_6, 298 K, plus apt): δ 189.1 (t, J_{P-C} = 6.4, Os−C), 174.1 (s, NCN), 152.8 (s, C_q), 146.4 (s, CH Ph), 140.3, 131.6 (both s, C_q), 128.7, 126.5, 125.6, 124.9, 124.8, 121.9, 119.1 (all s, CH Ph and benzothiazole), 27.3 (vt, N = 23.6, $PCH(CH_3)_2$), 19.9, 19.7 (both s, $PCH(CH_3)_2$). $T_{1(min)}$ (ms, OsH, 300 MHz, C_7D_8, 233 K): 94 (−11.48 ppm).

Structural Analysis of Complexes 2 and 4. Crystals suitable for the X-ray diffraction were obtained by slow diffusion of pentane into concentrated solutions of the complexes in toluene. X-ray data were collected on Bruker Smart APEX or APEX DUO difractometers equipped with a normal focus, 2.4 kW sealed tube source (Mo radiation, λ= 0.71073 Å) operating at 50 kV and 30 (**2**)/40 (**4**) mA. Data were collected over the complete sphere. Each frame exposure time was 10 s (**2**) or 30 s (**4**) covering 0.3° in ω.Data were corrected for absorption by using a multiscan method applied with the SADABS program.[43] The structures were solved by the Patterson (Os atoms) or direct methods and conventional Fourier techniques and refined by full-matrix least-squares on F^2 with SHELXL97.[44] Anisotropic parameters were used in the last cycles of refinement for all non-hydrogen atoms. Complex **4** crystallizes as a racemic twin (Flack parameter 0.348(18)) with a *quasi* C2 symmetry axes between the two osmium atoms. In this compound, the refined C−C distances in the two triisopropylphosphines were observed in the range 1.4−1.6 Å, and a model with the same C−C refined distance was preferred (1.52(1) Å). In addition, two molecules of pentane were observed in the asymmetric unit, which were refined with partial occupancies, restrained geometries and isotropic displacement parameters. The hydrogen atoms in both structures were observed or calculated and refined freely or using a restricted riding model. Hydride ligands were observed in the difference Fourier maps but refined to close to metals, so a restrained refinement fixing the OsH bond length to 1.59(1) Å (CCDC) was used. In **4**, the H(04)−H(05) distance was restrained to 1.3(1) Å, as observed in the theoretical calculations, because it does not converged properly. The agostic C(31)−H(31) bond distance was refined freely. The highest electronic residuals were observed in the close proximity of the metal centers and make no chemical sense.

Crystal data for **2**: $C_{27}H_{52}N_2OsP_2$, M_W 656.85, pale yellow, irregular block (0.20 × 0.20 × 0.12), orthorhombic, space group *Pbca*, a: 17.5141(7) Å, b: 14.3683(6) Å, c: 23.0704(9) Å, V = 5805.6(4) Å^3, Z = 8, D_{calc}: 1.503 g cm$^{−3}$, F(000): 2672, T = 100(2) K, μ 4.520 mm$^{−1}$. 51574 measured reflections (2θ: 4−56°, ω scans 0.3°), 7151 unique (R_{int} = 0.0344); minimum/maximum transmission factors 0.571/0.498. Final agreement factors were R^1 = 0.0202 (5555 observed reflections, I > 2σ(I)) and wR^2 = 0.0441; data/restraints/parameters 7151/3/317; GoF = 0.928. Largest peak and hole 1.177 and −0.704 e/Å^3.

Crystal data for **4**: $C_{49}H_{98}N_2Os_2P_4 \cdot C_5H_{12}$, M_W 1291.72, green, irregular block (0.18 × 0.03 × 0.03), monoclinic, space group *Cc*, a: 15.461(4)Å, b: 17.256(4)Å, c: 11.892(3)Å, β: 100.563(3)°, V = 3118.9(13)Å^3, Z = 2, Z' = 0.5, D_{calc}: 1.375g cm$^{−3}$, F(000): 1320, T = 100(2) K, μ 4.205 mm$^{−1}$. 13195 measured reflections (2θ: 4−56°, ω scans 0.3°), 6324 unique (R_{int} = 0.0280); minimum/maximum transmission factors 0.682/0.862. Final agreement factors were R^1 = 0.0298 (5608 observed reflections, I > 2σ(I)) and wR^2 = 0.0731; Flack parameter: 0.348(18), data/restraints/parameters 6324/60/343; GoF = 1.044. Largest peak and hole 1.549 and −0.617 e/Å^3.

Computational Details. Calculations were performed at the DFT level using the M06 functional[45] including an ultrafine integration grid, as implemented in Gaussian 09.[46] The Os atom was described using the scalar relativistic Stuttgart-Dresden SDD pseudopotential and its associated double-ζ basis set,[47] complemented with a set of f polarization functions.[48] The standard triple-ζ basis set 6-311G(d,p) basis set was used for the rest of atoms.[49] Calculation of the vibrational frequencies[50] at the optimized geometries showed that the compounds are minima on the potential energy surface This level is denoted M06/6-311G(d,p)&SDD(f).

Calculations of absorption spectra were accomplished in the present work using the time-dependent density functional theory (TD-DFT) method.[51] The assignment of the excitation energies to the experimental bands was performed on the basis of the energy values and oscillator strengths. The B3LYP Hamiltonian was chosen because it was proven to provide accurate structures and reasonable UV−vis spectra for a variety of chromophores[52] including organometallic complexes.[53] This level is denoted TD-B3LYP/6-311G(d,p)&SDD-(f)//M06/6-311+G(d,p)&SDD(f).

■ ASSOCIATED CONTENT

Ⓢ Supporting Information

Structural analysis of complexes **5** and **6**; high field $^1H\{^{31}P\}$ NMR spectra (400 MHz, C_7D_8) of complex **4** as a function of temperature, UV/vis, normalized emission, and excitation spectra for **2**, **3**, **5**, and **6**; HOMO−1, HOMO, and LUMO of compounds **2**, **3**, **5**, and **6**; HOMO, HOMO−1, and HOMO−2 of compounds **3** and **4**; cyclic voltammetry (CV) and Osteryoung square-wave voltammetry (SW) for complex **6**; and CIF file giving positional and displacement parameters, crystallographic data, and bond lengths and angles of compounds **2**, **4**, **5**, and **6**. The supplemental file om5b00174_si_002.xyz contains the computed Cartesian coordinates of all of the molecules reported in this study. The file may be opened as a text file to read the coordinates, or opened directly by a molecular modeling program such as Mercury (version 3.3 or later, http://www.ccdc.cam.ac.uk/pages/Home.aspx) for visualization. The Supporting Information is available free of charge on the ACS Publications website at DOI: 10.1021/acs.organomet.5b00174.

■ AUTHOR INFORMATION

Corresponding Authors
*E-mail for M.A.E.: maester@unizar.es.
*E-mail for M.A.S.: sierraor@ucm.es.

Notes
The authors declare no competing financial interests.

■ ACKNOWLEDGMENTS

■ REFERENCES

(1) (a) Shilov, A. E.; Shul'pin, G. B. *Chem. Rev.* **1997**, *97*, 2879−2932. (b) Crabtree, R. H. *J. Chem. Soc., Dalton Trans.* **2001**, 2437−2450. (c) Ritleng, V.; Sirlin, C.; Pfeffer, M. *Chem. Rev.* **2002**, *102*, 1731−1769. (d) Labinger, J. A.; Bercaw, J. E. *Nature* **2002**, *417*, 507−514. (e) Crabtree, R. H. *J. Organomet. Chem.* **2004**, *689*, 4083−4091. (f) Godula, K.; Sames, D. *Science* **2006**, *312*, 67−72. (g) Mkhalid, I. A. I.; Barnard, J. H.; Marder, T. B.; Murphy, J. M.; Hartwig, J. F. *Chem. Rev.* **2010**, *110*, 890−931. (h) Lyons, T. W.; Sanford, M. S. *Chem. Rev.* **2010**, *110*, 1147−1169. (i) Wencel-Delord, J.; Dröge, T.; Liu, F.; Glorius, F. *Chem. Soc. Rev.* **2011**, *40*, 4740−4761. (j) Kuhl, N.; Hopkinson, M. N.; Wencel-Delord, J.; Glorius, F. *Angew. Chem., Int. Ed.* **2012**, *51*, 10236−10254.

(2) (a) Ryabov, A. D. *Chem. Rev.* **1990**, *90*, 403−424. (b) Kakiuchi, F.; Murai, S. *Top. Organomet. Chem.* **1999**, *3*, 47−79. (c) Dyker, G. *Angew. Chem., Int. Ed.* **1999**, *38*, 1699−1712. (d) Colby, D. A.; Bergman, R. G.; Ellman, J. A. *Chem. Rev.* **2010**, *110*, 624−655. (e) Baudoin, O. *Chem. Soc. Rev.* **2011**, *40*, 4902−4911.

(3) See for example: (a) Barea, G.; Esteruelas, M. A.; Lledós, A.; López, A. M.; Oñate, E.; Tolosa, J. I. *Organometallics* **1998**, *17*, 4065−4076. (b) Barrio, P.; Castarlenas, R.; Esteruelas, M. A.; Lledós, A.; Maseras, F.; Oñate, E.; Tomàs, J. *Organometallics* **2001**, *20*, 442−452. (c) Barrio, P.; Castarlenas, R.; Esteruelas, M. A.; Oñate, E. *Organometallics* **2001**, *20*, 2635−2638. (d) Barrio, P.; Esteruelas, M. A.; Oñate, E. *Organometallics* **2004**, *23*, 1340−1348. (e) Eguillor, B.; Esteruelas, M. A.; Oliván, O.; Puerta, M. *Organometallics* **2008**, *27*, 445−450. (f) Esteruelas, M. A.; Masamunt, A. B.; Oliván, O.; Oñate, E.; Valencia, M. *J. Am. Chem. Soc.* **2008**, *130*, 11612−11613. (g) Esteruelas, M. A.; Forcén, E.; Oliván, M.; Oñate, E. *Organometallics* **2008**, *27*, 6188−6192. (h) Eguillor, B.; Esteruelas, M. A.; García-Raboso, J.; Oliván, M.; Oñate, E. *Organometallics* **2009**, *28*, 3700−3709. (i) Eguillor, B.; Esteruelas, M. A.; García-Raboso, J.; Oliván, M.; Oñate, E.; Pastor, I. M.; Peñafiel, I.; Yus, M. *Organometallics* **2011**, *30*, 1658−1667. (j) Alabau, R. G.; Eguillor, B.; Esler, J.; Esteruelas, M. A.; Oliván, M.; Oñate, E.; Tsai, J.-Y.; Xia, C. *Organometallics* **2014**, *33*, 5582−5596. (k) Bolaño, T.; Esteruelas, M. A.; Fernández, I.; Oñate, E.; Palacios, A.; Tsai, J.-Y.; Xia, C. *Organometallics* **2015**, *34*, 778−789.

(4) (a) Esteruelas, M. A.; Fernández, I.; Herrera, A.; Martín-Ortiz, M.; Martínez-Álvarez, R.; Oliván, M.; Oñate, E.; Sierra, M. A.; Valencia, M. *Organometallics* **2010**, *29*, 976−986. (b) Crespo, O.; Eguillor, B.; Esteruelas, M. A.; Fernández, I.; García-Raboso, J.; Gómez-Gallego, M.; Martín-Ortiz, M.; Oliván, M.; Sierra, M. A. *Chem. Commun.* **2012**, *48*, 5328−5330. (c) Esteruelas, M. A.; Fernández, I.; Gómez-Gallego, M.; Martín-Ortiz, M.; Molina, P.; Oliván, M.; Otón, F.; Sierra, M. A.; Valencia, M. *Dalton Trans.* **2013**, *42*, 3597−3608.

(5) (a) Barrio, P.; Esteruelas, M. A.; Oñate, E. *Organometallics* **2004**, *23*, 3627−3639. (b) Baya, M.; Eguillor, B.; Esteruelas, M. A.; Oliván, M.; Oñate, E. *Organometallics* **2007**, *26*, 6556−6563.

(6) Baya, M.; Eguillor, B.; Esteruelas, M. A.; Lledós, A.; Oliván, M.; Oñate, E. *Organometallics* **2007**, *26*, 5140−5152.

(7) Esteruelas, M. A.; Lahoz, F. J.; López, A. M.; Oñate, E.; Oro, L. A.; Ruiz, N.; Sola, E.; Tolosa, J. I. *Inorg. Chem.* **1996**, *35*, 7811−7817.

(8) Esteruelas, M. A.; García-Raboso, J.; Oliván, M. *Organometallics* **2011**, *30*, 3844−3852.

(9) (a) Esteruelas, M. A.; García-Raboso, J.; Oliván, M.; Oñate, E. *Inorg. Chem.* **2012**, *51*, 5975−5984. (b) Esteruelas, M. A.; García-Raboso, J.; Oliván, M. *Inorg. Chem.* **2012**, *51*, 9522−9528.

(10) Alós, J.; Bolaño, T.; Esteruelas, M. A.; Oliván, M.; Oñate, E.; Valencia, M. *Inorg. Chem.* **2013**, *52*, 6199−6213.

(11) See for example: (a) Rybak, J.-C.; Hailmann, M.; Matthes, P. R.; Zurawski, A.; Nitsch, J.; Steffen, A.; Heck, J. G.; Feldmann, C.; Götzendörfer, S.; Meinhardt, J.; Sextl, G.; Kohlmann, H.; Sedlmaier, S. J.; Schnick, W.; Müller-Buschbaum, K. *J. Am. Chem. Soc.* **2013**, *135*, 6896−6902. (b) Li, J.; Yang, G.; Hou, L.; Cui, L.; Li, Y.; Wang, Y.-Y.; Shi, Q.-Z. *Dalton Trans.* **2013**, *42*, 13590−13598. (c) Wang, S.; Xiong, S.; Wang, Z.; Du, J. *Chem.—Eur. J.* **2011**, *17*, 8630−8642 and references therein..

(12) Firmansyah, D.; Ciuciu, A. I.; Hugues, V.; Blanchard-Desce, M.; Flamigni, L.; Gryko, D. T. *Chem.—Asian J.* **2013**, *8*, 1279−1294.

(13) (a) Tao, T.; Ma, B.-B.; Peng, Y.-X.; Wang, X.-X.; Huang, W.; You, X.-Z. *J. Org. Chem.* **2013**, *78*, 8669−8679. (b) Tao, T.; Peng, Y.-X.; Huang, W.; You, X.-Z. *J. Org. Chem.* **2013**, *78*, 2472−2481. (c) Hu, B.; Fu, S.-J.; Xu, F.; Tao, T.; Zhu, H.-Y.; Cao, K.-S.; Huang, W.; You, X.-Z. *J. Org. Chem.* **2011**, *76*, 4444−4456. (d) Shikuma, J.; Mori, A.; Masui, K.; Matsuura, R.; Sekiguchi, A.; Ikegami, H.; Kawamoto, M.; Ikeda, T. *Chem.—Asian J.* **2007**, *2*, 301−305.

(14) (a) Ugorova, N. N.; Brovko, L. Y. *Luminescence* **2002**, *17*, 321−330. (b) Day, J. C.; Tisi, L. C.; Bailey, M. J. *Luminescence* **2004**, *19*, 8−20. (c) Nakatsu, T.; Ichiyama, S.; Hiratake, J.; Saldanha, A.; Kobashi, N.; Sakata, K.; Kato, H. *Nature* **2006**, *440*, 372−376.

(15) (a) Sun, X.; Zhao, Y.; Lin, V. S.-Y.; Slowing, I. I.; Trewyn, B. G. *J. Am. Chem. Soc.* **2011**, *133*, 18554−18557. (b) Yang, Y.; Shao, Q.; Deng, R.; Wang, C.; Teng, X.; Cheng, K.; Huang, L.; Liu, Z.; Liu, X.; Xing, B. *Angew. Chem., Int. Ed.* **2012**, *51*, 3125−3129. (c) Van de Bittner, G. C.; Bertozzi, C. R.; Chang, C. J. *J. Am. Chem. Soc.* **2013**, *135*, 1783−1795.

(16) (a) Lancaster, K. M.; Gerken, J. B.; Durrell, A. C.; Palmer, J. H.; Gray, H. B. *Coord. Chem. Rev.* **2010**, *254*, 1803−1811. (b) Bhaumik, C.; Das, S.; Saha, D.; Dutta, S.; Baitalik, S. *Inorg. Chem.* **2010**, *49*, 5049−5062. (c) Saha, D.; Das, S.; Mardanya, S.; Baitalik, S. *Dalton Trans.* **2012**, *41*, 8886−8898. (d) Li, Z.-Z.; Niu, Y.-L.; Zhou, H.-Y.; Chao, H.-Y.; Ye, B.-H. *Inorg. Chem.* **2013**, *52*, 10087−10095. (e) Das, S.; Karmakar, S.; Saha, D.; Baitalik, S. *Inorg. Chem.* **2013**, *52*, 6860−6879. (f) Maity, D.; Bhaumik, C.; Mondal, D.; Baitalik, S. *Dalton Trans.* **2014**, *43*, 1829−1845. (g) Das, S.; Karmakar, S.; Mardanya, S.; Baitalik, S. *Dalton Trans.* **2014**, *43*, 3767−3782.

(17) See for example: (a) Belliston-Bittner, W.; Dunn, A. R.; Nguyen, Y. H. L; Stuehr, D. J.; Winkler, J. R.; Gray, H. B. *J. Am. Chem. Soc.* **2005**, *127*, 15907−15915. (b) Lee, P. H.-M.; Ko, C.-C.; Zhu, N.; Yam,

V. W.-W. *J. Am. Chem. Soc.* **2007**, *129*, 6058−6059. (c) Tzeng, B.-C.; Chen, B.-S.; Chen, C.-K.; Chang, Y.-P.; Tzeng, W.-C.; Lin, T.-Y.; Lee, G.-H.; Chou, P.-T.; Fu, Y.-J.; Chang, A. H.-H. *Inorg. Chem.* **2011**, *50*, 5379−5388. (d) Henry, K. E.; Balasingham, R. G.; Vortherms, A. R.; Platts, J. A.; Valliant, J. F.; Coogan, M. P.; Zubieta, J.; Doyle, R. P. *Chem. Sci.* **2013**, *4*, 2490−2495.

(18) Recent examples: (a) Murphy, L.; Congreve, A.; Pålsson, L.-O.; Williams, J. A. G. *Chem. Commun.* **2010**, *46*, 8743−8745. (b) Li, S. P.-Y.; Tang, T. S.-M.; Yiu, K. S.-M.; Lo, K. K.-W. *Chem.—Eur. J.* **2012**, *18*, 13342−13354.

(19) (a) Schneider, J.; Lee, Y.-A.; Pérez, J.; Brennessel, W. W.; Flaschenriem, C.; Eisenberg, R. *Inorg. Chem.* **2008**, *47*, 957−968. (b) Lan, Y.-Q.; Li, S.-L.; Fu, Y.-M.; Xu, Y.-H.; Li, L.; Su, Z.-M.; Fu, Q. *Dalton Trans.* **2008**, 6796−6807. (c) Yue, C.; Yan, C.; Feng, R.; Wu, M.; Chen, L.; Jiang, F.; Hong, M. *Inorg. Chem.* **2009**, *48*, 2873−2879. (d) Li, Z.; Dellali, A.; Malik, J.; Motevalli, M.; Nix, R. M.; Olukoya, T.; Peng, Y.; Ye, H.; Gillin, W. P.; Hernández, I.; Wyatt, P. B. *Inorg. Chem.* **2013**, *52*, 1379−1387.

(20) Some examples: (a) Henary, M. M.; Wu, Y. G.; Fahrni, C. J. *Chem.—Eur. J.* **2004**, *10*, 3015−3025. (b) Kim, S. J.; Kool, E. T. *J. Am. Chem. Soc.* **2006**, *128*, 6164−6171. (c) Rouffet, M.; de Oliveira, C. A. F.; Udi, Y.; Agrawal, A.; Sagi, I.; McCammon, J. A.; Cohen, S. M. *J. Am. Chem. Soc.* **2010**, *132*, 8232−8233 See also refs 15b and 16c.

(21) (a) Yu, G.; Yin, S.; Liu, Y.; Shuai, Z.; Zhu, D. *J. Am. Chem. Soc.* **2003**, *125*, 14816−14824. (b) Xu, X.; Liao, Y.; Yu, G.; You, H.; Di, C.; Su, Z.; Ma, D.; Wang, Q.; Li, S.; Wang, S.; Ye, J.; Liu, Y. *Chem. Mater.* **2007**, *19*, 1740−1748. (c) Hung, W.-Y.; Chi, L.-C.; Chen, W.-J.; Chen, Y.-M.; Chou, S.-H.; Wong, K.-T. *J. Mater. Chem.* **2010**, *20*, 10113−10119. (d) Hung, W.-Y.; Chi, L.-C.; Chen, W.-J.; Mondal, E.; Chou, S.-H.; Wong, K.-T.; Chi, Y. *J. Mater. Chem.* **2011**, *21*, 19249−19256. (e) Mondal, E.; Hung, W.-Y.; Chen, Y.-H.; Cheng, M.-H.; Wong, K.-T. *Chem.—Eur. J.* **2013**, *19*, 10563−10572.

(22) For luminescent osmium compounds containing a coordinated benzimidazole moiety see: (a) Saha, D.; Das, S.; Maity, D.; Dutta, S.; Baitalik, S. *Inorg. Chem.* **2011**, *50*, 46−61. (b) Maity, D.; Bhaumik, C.; Mondal, C.; Baitalik, S. *Inorg. Chem.* **2013**, *52*, 13941−13955.

(23) See for example: (a) Esteruelas, M. A.; Lledós, A.; Oliván, M.; Oñate, E.; Tajada, M. A.; Ujaque, G. *Organometallics* **2003**, *22*, 3753−3765. (b) Baya, M.; Esteruelas, M. A.; González, A. I.; López, A. M.; Oñate, E. *Organometallics* **2005**, *24*, 1225−1232. (c) Buil, M. L.; Esteruelas, M. A.; Goni, E.; Oliván, M.; Oñate, E. *Organometallics* **2006**, *25*, 3076−3083. (d) Bolaño, T.; Castarlenas, R.; Esteruelas, M. A.; Oñate, E. *J. Am. Chem. Soc.* **2006**, *128*, 3965−3973.

(24) See for example: (a) Esteruelas, M. A.; Gutiérrez-Puebla, E.; López, A. M.; Oñate, E.; Tolosa, J. I. *Organometallics* **2000**, *19*, 275−284. (b) Baya, M.; Esteruelas, M. A.; Oñate, E. *Organometallics* **2001**, *20*, 4875−4886. (c) Esteruelas, M. A.; González, A. I.; López, A. M.; Oñate, E. *Organometallics* **2003**, *22*, 414−425. (d) Esteruelas, M. A.; Hernández, Y. A.; López, A. M.; Oliván, M.; Oñate, E. *Organometallics* **2005**, *24*, 5989−6000. (e) Cerón-Camacho, R.; Morales-Morales, D.; Hernandez, S.; Le Lagadec, R.; Ryabov, A. D. *Inorg. Chem.* **2008**, *47*, 4988−4995.

(25) (a) Custelcean, R.; Jackson, J. E. *Chem. Rev.* **2001**, *101*, 1963−1980. (b) Epstein, L. M.; Shubina, E. S. *Coord. Chem. Rev.* **2002**, *231*, 165−181. (c) Belkova, N. V.; Shubina, E. S.; Epstein, L. M. *Acc. Chem. Res.* **2005**, *38*, 624−631.

(26) (a) Wessel, J.; Lee, J. C., Jr.; Peris, E.; Yap, G. P. A.; Fortin, J. B.; Ricci, J. S.; Sini, G.; Albinati, A.; Koetzle, T. F.; Einsenstein, O.; Rheingold, A. L.; Crabtree, R. H. *Angew. Chem., Int. Ed.* **1995**, *34*, 2507−2509. (b) Patel, B. P.; Wessel, J.; Yao, W.; Lee, J. C., Jr.; Peris, E.; Koetzle, T. F.; Yap, G. P. A; Fortin, J. B.; Ricci, J. S.; Sini, G.; Albinati, A.; Einsenstein, O.; Rheingold, A. L.; Crabtree, R. H. *New. J. Chem.* **1997**, *21*, 413−421. (c) Gusev, D. G.; Lough, A. J.; Morris, R. H. *J. Am. Chem. Soc.* **1998**, *120*, 13138−13147. (d) Abdur-Rashid, K.; Gusev, D. G.; Lough, A. J.; Morris, R. H. *Organometallics* **2000**, *19*, 834−843. (e) Belkova, N. V.; Shubina, E. S.; Gutsul, E. I.; Epstein, L. M.; Eremenko, I. L.; Nefedov, S. E. *J. Organomet. Chem.* **2000**, *610*, 58−70. (f) Abdur-Rashid, K.; Lough, A. J.; Morris, R. H. *Can. J. Chem.* **2001**, *79*, 964−976.

(27) Nonbonding H···H contacts are normally about twice the van der Waals radius of H or 2.4 Å. (a) Lee, J. C., Jr.; Rheingold, A. L.; Muller, B.; Pregosin, P. S.; Crabtree, R. H. *J. Chem. Soc., Chem. Commun.* **1994**, 1021−1022. (b) Lee, J. C., Jr.; Peris, E.; Rheingold, A. L.; Crabtree, R. H. *J. Am. Chem. Soc.* **1994**, *116*, 11014−11019. (c) Peris, E.; Lee, J. C., Jr.; Rambo, J. R.; Eisenstein, O.; Crabtree, R. H. *J. Am. Chem. Soc.* **1995**, *117*, 3485−3491. (d) Crabtree, R. H.; Eisenstein, O.; Sini, G.; Peris, E. *J. Organomet. Chem.* **1998**, *567*, 7−11. (e) Crabtree, R. H. *J. Organomet. Chem.* **1998**, *557*, 111−115.

(28) Toluene-d_8 was selected as solvent by its low polarity.

(29) (a) Valentini, M.; Pregosin, P. S.; Rüegger, H. *Organometallics* **2000**, *19*, 2551−2555. (b) Keresztes, I.; Williard, P. G. *J. Am. Chem. Soc.* **2000**, *122*, 10228−10229. (c) Barberá, J.; Puig, L.; Romero, P.; Serrano, J. L.; Sierra, T. *J. Am. Chem. Soc.* **2006**, *128*, 4487−4492.

(30) Kaucher, M. S.; Lam, Y.-F.; Pieraccini, S.; Gotarelli, G.; Davis, J. T. *Chem.—Eur. J.* **2005**, *11*, 164−173.

(31) The pK_a values are 4.51 for 2-phenylbenzimidazole and 6.39 for 2-phenylimidazole. See: Hofman, K. *Imidazole and its derivatives*; Interscience Publishers: New York, 1953.

(32) Balcells, D.; Clot, E.; Eisenstein, O. *Chem. Rev.* **2010**, *110*, 749−823.

(33) (a) Esteruelas, M. A.; Lahoz, F. J.; Oñate, E.; Oro, L. A.; Sola, E. *J. Am. Chem. Soc.* **1996**, *118*, 89−99. (b) Castarlenas, R.; Esteruelas, M. A.; Oñate, E. *Organometallics* **2000**, *19*, 5454−5463. (c) Wen, T. B.; Zhou, Z. Y.; Lau, C.-P.; Jia, G. *Organometallics* **2000**, *19*, 3466−3468. (d) Castarlenas, R.; Esteruelas, M. A.; Oñate, E. *Organometallics* **2001**, *20*, 3283−3292. (e) Castro-Rodrigo, R.; Esteruelas, M. A.; López, A. M.; Oñate, E. *Organometallics* **2008**, *27*, 3547−3555.

(34) Crabtree, R. H.; Holt, E. M.; Lavin, M.; Morehouse, S. M. *Inorg. Chem.* **1985**, *24*, 1986−1992.

(35) Lein, M. *Coord. Chem. Rev.* **2009**, *253*, 625−634.

(36) See for example: (a) Kubacek, P.; Hoffmann, R. *J. Am. Chem. Soc.* **1981**, *103*, 4320−4332. (b) Gusev, D. G.; Kuhlman, R.; Sini, G.; Eisenstein, O.; Caulton, K. G. *J. Am. Chem. Soc.* **1994**, *116*, 2685−2686. (c) Gusev, D. G.; Kuhlman, R.; Rambo, J. R.; Berke, H.; Eisenstein, O.; Caulton, K. G. *J. Am. Chem. Soc.* **1995**, *117*, 281−292. (d) Kulhman, R.; Gusev, D. G.; Eremeko, I. L.; Berke, H.; Huffman, J. C.; Caulton, K. G. *J. Organomet. Chem.* **1997**, *536−537*, 139−147. (e) Kulhman, R.; Clot, E.; Leforestier, C.; Streib, W. E.; Eisenstein, O.; Caulton, K. G. *J. Am. Chem. Soc.* **1997**, *119*, 10153−10169.

(37) Baya, M.; Esteruelas, M. A.; Oñate, E. *Organometallics* **2011**, *30*, 4404−4408.

(38) (a) Aracama, M.; Esteruelas, M. A.; Lahoz, F. J.; Lopez, J. A.; Meyer, U.; Oro, L. A.; Werner, H. *Inorg. Chem.* **1991**, *30*, 288−293. (b) Atencio, R.; Esteruelas, M. A.; Lahoz, F. J.; Oro, L. A.; Ruiz, N. *Inorg. Chem.* **1995**, *34*, 1004−1006. (c) Kulhman, R.; Streib, W. E.; Huffman, J. C.; Caulton, K. G. *J. Am. Chem. Soc.* **1996**, *118*, 6934−6945. (d) Wolf, J.; Stuer, W.; Grünwald, C.; Gevert, O.; Laubender, M.; Werner, H. *Eur. J. Inorg. Chem.* **1998**, 1827−1834. (e) Bhattacharya, S.; Gupta, P.; Basoli, F.; Pierport, C. G. *Inorg. Chem.* **2002**, *41*, 5810−5816.

(39) Navon, G.; Sutin, N. *Inorg. Chem.* **1974**, *13*, 2159−2164.

(40) Forster, L. S. *Coord. Chem. Rev.* **2006**, *250*, 2023−2033.

(41) Costa, P. J.; Calhorda, M. J. *Inorg. Chim. Acta* **2006**, *359*, 3617−3624.

(42) Xu, M.-L.; Zhou, R.; Wang, G.-J.; Yu, J.-Y. *Inorg. Chim. Acta* **2009**, *362*, 515−518.

(43) Blessing, R. H. *Acta Crystallogr.* **1995**, *A51*, 33−38. SADABS: Area-detector absorption correction; Bruker-AXS,: Madison, WI, 1996.

(44) SHELXTL Package v. 6.10; Bruker-AXS: Madison, WI, 2000. Sheldrick, G. M. *Acta Crystallogr.* **2008**, *A64*, 112−122.

(45) Zhao, Y.; Truhlar, D. *Theor. Chem. Acc.* **2008**, *120*, 215−241.

(46) *Gaussian 09*, Revision B.01; Frisch, M. J.; Trucks, G. W.; Schlegel, H. B.; Scuseria, G. E.; Robb, M. A.; Cheeseman, J. R.; Scalmani, G.; Barone, V.; Mennucci, B.; Petersson, G. A.; Nakatsuji, H.; Caricato, M.; Li, X.; Hratchian, H. P.; Izmaylov, A. F.; Bloino, J.; Zheng, G.; Sonnenberg, J. L.; Hada, M.; Ehara, M.; Toyota, K.; Fukuda, R.; Hasegawa, J.; Ishida, M.; Nakajima, T.; Honda, Y.; Kitao, O.; Nakai, H.; Vreven, T.; J. A., Jr. Montgomery, Peralta, J. E.; Ogliaro,

F.; Bearpark, M.; Heyd, J. J.; Brothers, E.; Kudin, K. N.; Staroverov, V. N.; Kobayashi, R.; Normand, J.; Raghavachari, K.; Rendell, A.; Burant, J. C.; Iyengar, S. S.; Tomasi, J.; Cossi, M.; Rega, N.; Millam, N. J.; Klene, M.; Knox, J. E.; Cross, J. B.; Bakken, V.; Adamo, C.; Jaramillo, J.; Gomperts, R.; Stratmann, R. E.; Yazyev, O.; Austin, A. J.; Cammi, R.; Pomelli, C.; Ochterski, J. W.; Martin, R. L.; Morokuma, K.; Zakrzewski, V. G.; Voth, G. A.; Salvador, P.; Dannenberg, J. J.; Dapprich, S.; Daniels, A. D.; Ö. Farkas, Foresman, J. B.; Ortiz, J. V.; Cioslowski, J.; Fox, D. J., Gaussian, Inc.: Wallingford, CT, 2009.

(47) Andrae, D.; Haeussermann, U.; Dolg, M.; Stoll, H.; Preuss, H. *Theor. Chim. Acta* **1990**, *77*, 123−141.

(48) Ehlers, A. W.; Bohme, M.; Dapprich, M. S.; Gobbi, A.; Hollwarth, A.; Jonas, V.; Kohler, K. F.; Stegmann, R.; Veldkamp, A.; Frenking, G. *Chem. Phys. Lett.* **1993**, *208*, 111−114.

(49) Hehre, W. J.; Ditchfield, R.; Pople, J. A. *J. Chem. Phys.* **1972**, *56*, 2257−2261.

(50) Iver, J. W.; Komornicki, A. K. *J. Am. Chem. Soc.* **1972**, *94*, 2625−2633.

(51) (a) Casida, M. E. *Recent Developments and Applications of Modern Density Functional Theory*; Elsevier: Amsterdam, 1996; Vol. *4*. (b) Casida, M. E. In *Recent Advances in Density Functional Methods*; Chong, D. P., Ed.; World Scientific: Singapore, 1995; Vol. *1*, pp 155−192.

(52) For a review, see: Dreuw, A.; Head-Gordon, M. *Chem. Rev.* **2005**, *105*, 4009−4037.

(53) Recent examples: (a) Nemykin, V. N.; Makarova, E. A.; Grosland, J. O.; Hadt, R. G.; Koposov, A. Y. *Inorg. Chem.* **2007**, *46*, 9591−9601. (b) Santi, S.; Orian, L.; Donoli, A.; Durante, C.; Bisello, A.; Ganis, P.; Ceccon, A.; Crociani, L.; Benetollo, F. *Organometallics* **2007**, *26*, 5867−5879. (c) Lage, M. L.; Fernández, I.; Mancheño, M. J.; Sierra, M. A. *Inorg. Chem.* **2008**, *47*, 5253−5258. (d) López-Alberca, M. P.; Mancheño, M. J.; Fernández, I.; Gómez-Gallego, M.; Sierra, M. A.; Torres, R. *Chem.—Eur. J.* **2009**, *15*, 3595−3603. (e) Lage, M. L.; Fernández, I.; Mancheño, M. J.; Sierra, M. A. *Chem.—Eur. J.* **2010**, *16*, 6616−6624. (f) Chu, G. M.; Fernández, I.; Sierra, M. A. *Chem.—Eur. J.* **2013**, *19*, 5899−5908.